

This item is the archived peer-reviewed author-version of:

fMRI reveals a novel region for evaluating acoustic information for mate choice in a female songbird

Reference:

Van Ruijssevelt Lisbeth, Chen Yining, van Eugen Karl, Hamaide Julie, de Groof Geert, Verhoye Marleen, Güntürkün Onur, Woolley Sarah C., Van Der Linden Anne-Marie.- fMRI reveals a novel region for evaluating acoustic information for mate choice in a female songbird
Current biology - ISSN 0960-9822 - 28:5(2018), e6
Full text (Publisher's DOI): <https://doi.org/10.1016/J.CUB.2018.01.048>
To cite this reference: <https://hdl.handle.net/10067/1494590151162165141>

1 **fMRI reveals a novel region for evaluating**
2 **acoustic information for mate choice**
3 **in a female songbird**

4 **Author list and affiliations**

5 Lisbeth Van Ruijssevelt¹, Yining Chen², Kaya von Eugen³, Julie Hamaide¹, Geert De Groof¹, Marleen
6 Verhoye¹, Onur Güntürkün³, Sarah C. Woolley^{2,4*}, and Annemie Van der Linden^{1,4,5*}

7 ¹ Bio-Imaging lab, Department of Biomedical Sciences, University of Antwerp, 2610 Antwerpen, Belgium

8 ² Department of Biology, McGill University, Montreal QC H3A 1B1, Canada

9 ³ AE Biopsychologie, Fakultät für Psychologie, Ruhr-Universität Bochum, 44801 Bochum, Germany

10 ⁴ These authors contributed equally

11 ⁵ Lead contact

12 ***Correspondence**

13 **Annemie Van der Linden:** Annemie.vanderlinden@uantwerpen.be

14 **Sarah C. Woolley:** sarah.woolley@mcgill.ca

Gewijzigde veldcode

Gewijzigde veldcode

15 SUMMARY

16 Selection of sexual partners is among the most critical decisions individuals make and is therefore strongly
17 shaped by evolution. In social species, where communication signals can convey substantial information
18 about the identity, state, or quality of the signaler, accurate interpretation of communication signals for
19 mate choice is crucial. Despite the importance of social information processing, to date relatively little is
20 known about the neurobiological mechanisms that contribute to ~~natural-social-sexual~~ decision-making
21 and preferences. In this study, we used a combination of whole brain functional magnetic resonance
22 imaging (fMRI), immediate early gene expression, and behavior tests to identify the circuits important for
23 the perception and evaluation of courtship song in a female songbird, the zebra finch (*Taeniopygia*
24 *guttata*). Female zebra finches are sensitive to subtle differences in male song performance and strongly
25 prefer the longer, faster, and more stereotyped courtship songs to non-courtship renditions. Using BOLD
26 fMRI, and ~~with-as~~ further validation, ~~using~~ EGR1 expression assays, we uncovered a novel region involved
27 in auditory perceptual decision-making in a sensory integrative region of the ~~avian~~ central nidopallium
28 outside the traditionally studied auditory forebrain pathway. Changes in activity in this region in response
29 to acoustically similar but categorically divergent stimuli showed stronger parallels to behavioral
30 responses than an auditory sensory region. These data highlight a potential role for the caudocentral
31 nidopallium (NCC) as a novel node in the avian circuitry underlying the evaluation of acoustic signals and
32 their use in mate choice.

33 KEYWORDS

34 Auditory perception; mate choice; zebra finches; songbirds; functional MRI; auditory fMRI; courtship
35 song; directed song

36 INTRODUCTION

37 Sexual selection potently shapes both the production and perception of courtship signals across species
38 [1, 2]. In order to be effective, courtship signals must be accurately detected and perceived, and
39 consequently the sensory and even cognitive systems of receivers critically influence the evolution of
40 signal production in response to sexual selection by mate choice [3, 4]. For example, in Tungara frogs, the
41 spectral properties of advertisement calls match the tuning properties of the peripheral auditory end
42 organs of receivers, indicating that the properties of receiver's auditory systems may have shaped the
43 evolution of advertisement calls [5, 6]. At the same time, female Tungara frog cognitive discrimination
44 abilities have been proposed to constrain call elaboration and complexity [7]. In songbirds, female birds
45 can exert acute influences on the learning and production of song by males. For example, female cowbirds
46 use rapid motor displays to indicate to juvenile males which elements to retain in their song repertoire
47 [8-10]. Thus, the sensory and cognitive biases of female receivers can shape signal production even in the
48 context of a culturally transmitted trait. Despite the importance of female perceptual and cognitive
49 systems for mate choice and signal evolution, there is a surprising lack of knowledge on the neural
50 mechanisms that contribute to ~~natural-social~~sexual decision-making and preferences.

51 Songbirds are a classic model for studying the neural basis of vocal communication. In many species, males
52 produce a complex, learned vocalization, the song, which conveys substantial information about the
53 identity, state, and quality of the signaler [11, 12]. and both song learning and production depend on
54 specialized neural circuitry known as the 'song system' [Brainard and Doupe, 2005; Mooney, 2009]. Song
55 is a key trait used in mate-choice decisions, and female receivers must thus accurately assess and interpret
56 the information song provides. In zebra finches, females show preferences for the songs of different males
57 as well as for songs performed in different social contexts [13-18]. For example, females prefer the longer,
58 faster, and more stereotyped courtship song ~~males direct specifically to them~~ ('female directed' or FD
59 song), over song performed when a male is alone ('undirected' or UD song), even when the song is from
60 an unfamiliar singer [17, 19]. However, while female song preferences have been the focus of
61 considerable study, little is known about the specific neural circuits in females, especially circuits beyond
62 the canonical auditory system, that are necessary for the perception of, preference for, and response to
63 courtship signals.

64 One challenge in the study of neural processes of song preference is that most methods commonly used
65 in songbird research require the *a priori* selection of particular region(s) of interest (ROIs), and, in many

Met opmerkingen [scw1]: Brainard MS, Doupe AJ. What songbirds teach us about learning. *Nature*. 2002 May 16;417(6886):351-8.

Met opmerkingen [scw2]: Mooney R. Neurobiology of song learning. *Current opinion in neurobiology*. 2009 Dec 31;19(6):654-60.

66 [eases, often involve](#) comparison between individuals that have heard different stimuli. While this
67 approach works well on identified circuits like the classical auditory pathway, it has limited ability to
68 uncover novel ROIs. In contrast, functional magnetic resonance imaging (fMRI) can infer neural activity at
69 the level of the whole brain and differential neural responses to a range of different stimuli can be
70 investigated within a single individual. Therefore, we used blood-oxygen level dependent (BOLD) fMRI –
71 which has previously been successfully implemented in songbirds [20-23] – to elucidate the neural
72 substrates of the processing of FD songs at the level of the whole brain in female zebra finches. Our fMRI
73 data, validated by immunocytochemistry (ICC), [identify-identified](#) two regions selectively activated by FD
74 versus UD song. The pattern of activity in one of these regions, the caudocentral nidopallium (NCC),
75 paralleled the behavioral responses of females. In contrast, activity in an auditory sensory region, the
76 caudomedial mesopallium (CMM), was similar in response to songs with shared temporal acoustic
77 patterns. Thus, to our knowledge, these are the first data to identify a potential role of the NCC as a novel
78 node in the avian circuitry underlying the evaluation of acoustic signals and their use in mate choice.

79 RESULTS

80 fMRI reveals two forebrain regions with greater activation in response to FD song

81 Previous investigation of the neural circuits important for song perception and preference have focused
82 on a limited subset of mainly auditory regions in the songbird caudal forebrain. To search more broadly
83 for regions differentially affected by variation in [song-the performance-acoustic features of song driven](#)
84 [by changes in related to](#) social context, we used fMRI to assess neural activity across forebrain regions in
85 adult female zebra finches in response to unfamiliar FD and UD song stimuli. In line with previous studies
86 (e.g. [24-27]), song playback elicited robust auditory responses, evidenced by reproducible BOLD signals,
87 in the auditory forebrain (analogous to the mammalian auditory cortex) including the primary auditory
88 area Field L and (parts of) the secondary auditory areas caudomedial mesopallium (CMM) and
89 caudomedial nidopallium (NCM) (Figure 1 and Supplementary figure S1A).

90 However, while auditory responses were widespread, only a limited subset of forebrain regions
91 responded differentially to the social context-[dependent variation in the acoustic features](#) of the stimulus.
92 Specifically, voxel-based analysis of the data revealed two clusters of voxels, one in the auditory CMM and
93 one in a multisensory integrative forebrain area the caudocentral nidopallium (NCC), which both exhibited
94 a higher BOLD response to FD song versus UD song (paired t-test). In the auditory forebrain, we found a

95 cluster of 10 significant voxels in the CMM ($T_{\max} = 4.3621$, $p_{\text{uncorr}}=0.0002$; Figure 2A-D; [one voxel = 0.125 x](#)
96 [0.125 x 0.400 mm³](#)), lateralized to the right hemisphere. We also discovered a second significant cluster
97 of 37 significant voxels, lateralized to the left hemisphere, within a portion of the multisensory integrative
98 forebrain region the NCC ($T_{\max} = 5.8893$, $p_{\text{uncorr}}<0.0001$; Figure 2E-H). Here, we only detected positive BOLD
99 responses (versus rest; $p_{\text{uncorr}}<0.001$) to FD song, but not to UD song. Thus, the voxel-based analysis
100 identified two regions with selectivity for FD song and, in both regions, the FD selectivity was exclusively
101 in one hemisphere.

102 Given ~~this~~ striking laterality of the selectivity for FD song (e.g. Figure 2A, E), we further investigated
103 the hemispheric difference using an ROI approach (see Methods). For this, we compared the average
104 BOLD responses to FD and UD song directly between the FD song selective clusters in the dominant
105 hemisphere versus their counterparts in the opposite hemisphere. We found a significant interaction of
106 stimulus and hemisphere in both the CMM ($F_{(1,16)}=7.8557$, $p=0.0128$) and [the](#) NCC ($F_{(1,16)}=10.7059$,
107 $p=0.0048$) (Figure 3). Similar to the voxel based analysis, this interaction indicates that FD song induces
108 significantly higher responses than UD song in the right CMM only ($p<0.0001$). In contrast, for the NCC
109 only the left hemisphere demonstrated significantly higher responses for FD versus UD song ($p<0.0001$).
110 In addition, the response to FD song in the NCC was higher in the left hemisphere than the right
111 hemisphere ($p=0.0170$). ~~Further,~~ [Further, to confirm FD selectivity and response lateralization in these](#)
112 [areas, we also applied](#) the ROI approach ~~was applied~~ to responses to pure tone stimuli in CMM and NCC
113 ~~in order to confirm FD selectivity and response lateralization in these areas~~. Responses to the pure tone
114 stimuli ~~appeared, similar to responses to UD song (CMM p=0.7657; NCC p=0.6227), were~~ significantly
115 lower than the responses to FD song in both regions (Figure S1B,C; CMM $p=0.0114$; NCC $p=0.0035$) ~~and~~
116 [were similar to responses to UD song \(CMM p=0.7657; NCC p=0.6227\)](#). Moreover, there was no apparent
117 lateralization of the responses to pure tones in either the CMM ($F_{(1,16)}=1.4537$, $p=0.2455$) ~~nor~~ the NCC
118 ($F_{(1,16)}=2.3910$, $p=0.1416$; Figure S1D,E). Thus, the ROI based analysis confirmed the FD song selectivity in
119 CMM and NCC and the specific lateralization of these FD song selective responses as determined earlier
120 in the ~~voxel-voxel~~-based analysis.

121 **EGR1 expression patterns in the CMM and the NCC support fMRI results**

122 The finding that the CMM and NCC display a selective BOLD activation pattern [dependent on the social](#)
123 [context for the courtship compared to the non-courtship song-of-song](#) suggests the involvement of these
124 two regions in female preference for FD song. One caveat with fMRI data, however, is that anesthesia is

125 used during scanning, which could affect the gain and selectivity of auditory responses (e.g. [30-32]). To
126 provide additional verification of the effects seen with fMRI, we quantified the expression of the
127 immediate early gene (IEG) EGR1 in the CMM and NCC after birds listened to FD or UD song while awake,
128 as an alternative marker for neuronal activation.

129 In general, EGR1 expression in both the CMM and NCC mirrored the fMRI results (Figure 4). In the CMM,
130 there was auditory-evoked EGR1 expression, with greater expression to song playback compared to
131 silence (Figure 4A; Figure S2; $F_{(1,14,6)}=33.3824$, $p<0.0001$). In addition, EGR1 expression was significantly
132 modulated by the [social-context-of-the](#) stimulus ($F_{(1,9,1)}=6.9585$; $p=0.0267$) with significantly higher
133 expression, bilaterally, in response to FD song versus UD song. As was the case for the BOLD fMRI
134 response, in the NCC there was no significant increase in EGR1 expression in response to song playback
135 compared to silence ($F_{(1,10,2)}=3.3582$, $p=0.0962$). However, EGR1 expression was significantly influenced
136 by the [social-context-of-the](#) song stimulus ($F_{(1,10,7)}=6.6228$, $p=0.0264$), with higher expression in response
137 to FD compared to UD song, which again parallels the fMRI results. Finally, in line with the results of the
138 lateralization analysis of the fMRI data, EGR1 expression in the NCC was strongly lateralized, with
139 significantly higher expression in the left compared to the right hemisphere ($F_{(1,4,6)}=8.2804$, $p=0.0379$).

140 **The NCC has lower tyrosine hydroxylase⁺-fiber density than the neighboring** 141 **nidopallium**

142 Through the fMRI and ICC data described above, we have uncovered a novel region within the
143 caudocentral nidopallium that shows selective activation for preferred, socially modulated song. In a
144 recently published songbird atlas, this region has been described as the caudolateral nidopallium (NCL),
145 stemming from its location lateral to the secondary auditory region NCM [29]. In pigeons and crows, a
146 portion of the NCL (which we will term the functional NCL) is significantly involved in executive functions,
147 such as decision-making and higher-order multimodal processing, and is considered functionally
148 analogous to the mammalian prefrontal cortex [33, 34]. The NCL in pigeons was identified based on its
149 connectivity, including a dense projection from midbrain tyrosine hydroxylase (TH⁺) neurons [35]. In
150 particular, compared to the surrounding nidopallium, the functional NCL contains more TH⁺ fibers in
151 general, as well as significantly more basket-like structures, visible as TH⁺ fibers coiling up around large
152 unstained perikarya (-Figure 5C black arrows; [36]) To investigate whether the FD song-selective region
153 that we identified using BOLD fMRI is comparable to the functional NCL in pigeons, we imaged the density

154 of TH⁺ fibers in the FD song-selective region and surrounding nidopallium, including the NCM and dorsal
155 and lateral caudal nidopallium (NC).

156 We observed clear variation in the density of TH⁺ fibers and baskets throughout the NC at the rostro-
157 caudal level of the ROI for our NCC fMRI signal (Figure 5A,B). The highest TH density, both in terms of
158 fibers and baskets, was found in the most medial region which corresponds to the most medial portions
159 of the NCM (Figure 5B,C top), and stretches laterally to approximately 1 mm from the midline. In the
160 central part of the NC directly lateral to the NCM (marked 'NCL' in the Karten atlas [29]) we found two
161 distinct areas based on their TH profile. A dorsal region, near the HVC, contained both TH baskets and
162 TH⁺-fiber innervation, although at lower levels than those observed in the NCM. Previous studies in zebra
163 finches have referred to this region as dorsal NCL (dNCL) [37, 38]. In contrast, a ventral region adjacent to
164 the arcopallium, where our FD song selective region was located, was only sparsely innervated by TH⁺
165 fibers and contained a low number of TH baskets (Figure 5C bottom). Based on this low level of TH⁺
166 innervation and baskets, it appears that the FD song-selective fMRI signal is not located in a functional
167 NCL-like region [36]. We therefore identify this region as the NCC given its neuroanatomical location.

168 **Neural selectivity in the NCC parallels behavioral responses to modified FD song**

169 Song-evoked activity, as measured by both fMRI and EGR1 expression, was modulated by the [social](#)
170 [context](#) of the stimulus in both the CMM and NCC. To gain further insight into how these two areas
171 compare in function, we tested behavioral and neural responses to two novel stimuli that manipulated
172 temporal and spectral song features: mFD songs which contained UD song syllables presented within the
173 temporal structure of FD song and mCTRL which contained FD song syllables presented within the
174 temporal structure of FD song to control for the overall song manipulation and greater amplitude contrast
175 of manipulated songs (Figure 6A).

176 We found striking differences in the BOLD fMRI responses between the CMM and NCC to the manipulated
177 stimuli. In the right CMM, BOLD responses to FD and the manipulated stimuli were similar and significantly
178 higher than responses to UD song (FD > UD: $T_{\max} = 3.0643$, $P_{FWE} = 0.0075$; mCTRL > UD: $T_{\max} = 3.3138$,
179 $P_{FWE} < 0.0040$; mFD > UD: $T_{\max} = 2.1620$, $P_{FWE} = 0.0538$; Figure 6B). In contrast, in the left NCC we observed
180 differential responses to the manipulated stimuli relative to the FD song. In particular, responses to FD
181 were not only significantly higher than responses to UD song, but also significantly higher than either
182 manipulated stimulus (FD > UD: $T_{\max} = 3.2424$, $P_{FWE} = 0.0139$; FD > mCTRL: $T_{\max} = 2.8184$, $P_{FWE} = 0.0367$;
183 FD > mFD: $T_{\max} = 2.8491$, $P_{FWE} = 0.0343$; Figure 6C). Thus, the CMM appears to respond to the manipulated

184 stimuli as similar to FD song, while the NCC distinguishes FD song from both the manipulated stimuli and
185 UD song.

186 To investigate whether CMM or NCC responses better correlate with behavioral perception of the
187 manipulated stimuli, we tested females on FD, UD, and manipulated stimuli in a call-back assay.
188 Behaviorally, females displayed dramatically different responses to the unmanipulated and manipulated
189 stimuli, as indicated by the significant main effect of stimulus ($F_{(3,33)}=3.0974$, $p=0.0400$; [Figure 6D](#)). In
190 particular, as has been seen in previous studies, females called significantly more to FD than UD songs
191 ($p=0.0287$; [17, 19]). In contrast, the preference for FD song diminished with both types of song
192 manipulation (manipulated songs vs. UD song: $p>0.20$).

193 Not only were responses to the manipulated stimuli diminished relative to FD song, they were also more
194 variable. In particular, while females consistently increased calling to FD song and decreased calling to UD
195 song, there was substantially more variation in the degree and direction of calling response to the
196 manipulated stimuli. To further investigate this variation, we compared the rankings of responses to
197 stimuli across females. For each female, we ranked the responses to each stimulus from most positive to
198 most negative. As we had noted in the raw data, FD song was more likely to receive the most positive
199 response (FD song was ranked '1' in 58% of the cases and was never ranked '4'; [Figure S3](#)). In contrast,
200 the second, third, and fourth ranks were almost equally likely to be any of the other stimuli. Overall, we
201 found that the pattern of rankings was significantly different for FD song compared to the UD song
202 (Cochran-Mantel-Haenszel $\chi^2=3.9302$, $p=0.0474$), and the mCTRL stimulus (Cochran-Mantel-Haenszel
203 $\chi^2=3.9302$, $p=0.0474$) and there was a trend toward a difference for mFD stimuli (Cochran-Mantel-
204 Haenszel $\chi^2=3.4571$, $p=0.0630$; [Figure S3](#)). However, there were no significant differences between the
205 rankings of UD song and either manipulated stimulus ([Figure S3](#); $p>0.20$). The variation across birds in the
206 responses to the manipulated stimuli indicates that females are sensitive to changes in auditory contrast
207 or other subtle differences present in the manipulated stimuli and furthermore these data imply that
208 females may not be categorizing the manipulated stimuli as FD song.

209 DISCUSSION

210 In social species, communication signals convey substantial information about the identity, state, or
211 quality of the signaler. During courtship, female receivers must accurately interpret male courtship signals
212 to judge their relevance for mate choice and to compose the proper behavioral response. In zebra finches,

213 females have been shown to be sensitive to subtle variation in male song and to strongly prefer the longer,
214 faster, and more stereotyped FD songs which are performed by males in a courtship context, to UD songs
215 which are sung when males are alone [17, 19]. While the study of the songbird auditory system has
216 identified regions that differentially respond to FD and UD song in females [17, 19], the role of other
217 forebrain regions in the discrimination and behavioral response to social context-induced ~~song~~-variation
218 [in the acoustic features of song](#), as well as the link between auditory responses and behavioral
219 preferences, remain poorly understood. Indeed, approaches used to study the neural basis of song
220 discrimination and preference to date often require the *a priori* selection of regions of interest, an
221 approach that is highly effective when used to study identified circuits, but not in uncovering novel regions
222 of interest. Here, we employed BOLD fMRI, ICC of activity dependent proteins, and behavioral assays to
223 uncover novel regions involved in song preference. Using fMRI, we identified two regions that
224 differentially respond to FD and UD song--: ~~One~~, the secondary auditory area CMM, ~~has previously been~~
225 ~~shown to be sensitive to natural variation in male song using EGR1 expression [17]. The second is and~~ a
226 novel region in the caudal nidopallium, the NCC. In both regions, ~~there was differential~~-EGR1 expression
227 ~~was modulated by the social context of the stimulus in~~ [response to FD and UD song](#), confirming the effects
228 seen in the BOLD fMRI responses. Interestingly, we found that the two regions differed in their responses
229 to manipulated stimuli. Relative to FD song, the manipulated stimuli elicited diminished behavioral
230 responses and BOLD fMRI signal in the NCC. These data hint that activity in the NCC may be more tightly
231 coupled to the behavioral response, and highlight the value of fMRI studies in songbirds for uncovering
232 novel circuits important for perception and behavior.

233 We used acoustically manipulated stimuli, created by interchanging either FD or UD syllables into the
234 temporal pattern of FD song, to probe differences in the function of the CMM versus the NCC. The mFD
235 stimuli thus contained UD spectral characteristics but FD temporal profiles whereas the mCTRL stimuli
236 contained both the spectral and temporal characteristics of FD song. Through the manipulation process,
237 we preserved the spectral characteristics of individual syllables as well as the mean and variance of the
238 ~~timing durations of syllables and~~ [inter](#) intersyllable intervals. However, both the mFD and mCTRL stimuli had
239 greater amplitude contrast at syllable onsets and offsets than did the unmanipulated stimuli. Intriguingly,
240 we observed that birds did not increase calling to either the mFD or the mCTRL stimulus indicating that
241 the manipulation diminished behavioral preferences for FD song. Moreover, whereas the FD song
242 received the most positive response from the majority of birds, the relative rankings of mFD, mCTRL, and
243 UD song were ~~both~~-lower and more variable than the [rankings of](#) FD song. Although, further song
244 manipulations are clearly needed to tease apart the influences of spectro-temporal and amplitude

245 features on song preference and perception, these data hint that the manipulated stimuli may be treated
246 as categorically different from FD song.

247

248 The behavioral responses are in striking contrast to the BOLD responses measured in the CMM, where
249 both manipulated stimuli resulted in similar activation profiles as the unmanipulated FD stimuli. Previous
250 studies comparing EGR1 expression in the CMM in response to salient or preferred songs, including FD
251 song in zebra finches [17, 19] as well as in response to ‘sexy-syllables’ in canaries [39] ~~has~~ have
252 hypothesized that [19, 40] the CMM is significantly involved in discriminating song quality or salience [17,
253 39]. However, one challenge has been the difficulty in uncoupling differences in acoustic features from
254 differences in preference. [17, 19, 39]. More recent work has demonstrated that EGR1 expression in the
255 CMM does not directly correlate with behavioral responses [19, 40]. Such a lack of correlation between
256 CMM response and behavior is similar to the effect that we report here. ~~Our findings,~~ based on the
257 responses to acoustically manipulated stimuli, where our data demonstrate that while neural responses
258 in the CMM are indeed sensitive to differences between FD and UD song in zebra finches, the neural
259 modulation does not neatly parallel the behavioral relevance of changes in acoustic structure. In
260 particular, we find that responses in the CMM are similar for FD song, mFD song which has the temporal
261 aspects of FD song but the spectral aspects of UD song (mFD), and mCTRL song, a control version of FD
262 song with greater amplitude contrast. As these three stimuli all share the same temporal features, we
263 hypothesize that in the CMM, the temporal pattern of the song may be more important than spectral
264 characteristics ~~to~~ in driving the increased activation seen for FD versus UD song. Note however that from
265 the current results, it is unclear whether the greater activation in the CMM in response to FD song is due
266 to the increased tempo of FD relative to UD song (e.g. shorter syllables) or due to greater song density
267 (e.g. shorter inter-motif intervals). In either case, the hypothesis that temporal features are more
268 important than spectral characteristics in driving CMM responses, is supported by the earlier observation
269 that EGR1 expression in the CMM is influenced by the temporal structure of song [41]. Moreover,
270 temporal cues have been shown to be more important than spectral cues in the processing of auditory
271 stimuli in the sensorimotor nucleus HVC (proper name; [42]), which raises the possibility that auditory
272 and sensorimotor forebrain circuits might be biased towards temporal features in this species in general
273 [43, 44].

274 Playback of FD song also selectively increased BOLD responses in the NCC. To our knowledge, this is the
275 first report of neural selectivity for socially modulated song outside of the classical avian auditory

276 pathway. Moreover, the pattern of activity in the NCC in response to the manipulated and unmanipulated
277 stimuli was remarkably similar to the pattern of behavioral preferences. In particular, both calling
278 behavior and the NCC BOLD responses were increased only in response to FD song playback. While it is
279 difficult to determine precisely which acoustic features drive or suppress the response to FD song, it is
280 interesting to speculate that both FD selectivity in the NCC and behavioral preferences may require the
281 preservation of intact ~~natural~~ song with all spectral and temporal components in place and natural
282 amplitude contrast at syllable on- and offsets. Additional studies that are more focused on elucidating the
283 effect of spectral and temporal variability on neural selectivity, and on how this correlates with behavioral
284 preference will be key in understanding how females weigh specific acoustic features when determining
285 song quality and ~~which-what~~ role ~~the~~ NCC in particular plays in this process. Moreover, one significant
286 caveat in the comparison of the fMRI and behavioral data is the difference in behavioral state: fMRI is
287 performed on anesthetized birds while birds are awake for behavioral tests. Such changes in state may
288 significantly affect the gain, latency, and tuning of neural responses [32, 94-96]. That said, the observed
289 parallels between responses in the NCC and behavioral preferences in this study, raise the intriguing
290 possibility that the NCC may be significant in driving behavioral responses to song.

291 The region we identify as the NCC in our fMRI images is located centrally in the caudal nidopallium and
292 exhibits lower levels of TH innervation than the surrounding nidopallium, including the NCM and the dNCL.
293 To our knowledge, there are no specific reports describing the function or connectivity of this region,
294 either in zebra finches or in any other songbird species. However, both the neuroanatomical position and
295 TH innervation profile of the identified FD song selective region are similar to the NCC, a higher-order
296 limbic forebrain area that has been described in a non-songbird avian species, the pigeon. In particular,
297 the connectivity of this region has been well-characterized in pigeons (Figure 7) and indicates that the
298 NCC may be involved in multiple facets of courtship behavior including coordinating auditory inputs,
299 memory from sexual imprinting structures, and vocal and behavioral responses to courtship signals. The
300 NCC receives auditory input from both the shell of the [auditory thalamic nucleus ovoidalis](#) (Ov shell) and
301 the [secondary cortical region](#) NCM (via the multimodal arcopallium), which is highly interconnected with
302 the CMM and the primary auditory forebrain [45-47]. In addition, the NCC is reciprocally connected to
303 regions implicated in learning and memory associated with sexual imprinting, such as the intermediate
304 medial nidopallium (NIM) and the limbic dorsal mesopallium (MD). Together, the connections to auditory
305 and imprinting structures raise the possibility that the NCC is a hub for the memorization and integration
306 of auditory and other sensory input which can influence mate choice in adult zebra finches [48-50]. Finally,
307 the NCC also connects to parts of the arcopallium with descending projections to motor output regions,

308 which may enable the NCC to modify behavioral responses [51]. In particular, with regard to our
309 behavioral assay, the NCC projects to the medial arcopallium (AM) which connects to the dorsomedial
310 nucleus (DM) of the midbrain via the posterior medial hypothalamus [51]. The DM can control brainstem
311 respiratory and vocal nuclei, and parts of DM have been shown to be involved in the control of female
312 reproductive behavior including copulation solicitation displays [46, 52-55]. Consequently, DM is a key
313 structure that could drive callback responses as well as increase copulation solicitation displays to
314 preferred songs. Thus, the connectivity of the NCC positions it as an integrative hub, potentially important
315 for evaluating courtship signals and coordinating a multi-faceted behavioral response. Our fMRI results,
316 documenting a correlation between neuronal responses in the NCC and behavioral callback responses to
317 acoustic stimuli, provide, to our knowledge, the first functional support of such a role for the NCC in the
318 evaluation of courtship signals and in coordinating resulting behavioral responses in female zebra finches.

319 The two independent techniques we used to infer neural activity each provide discrete, indirect measures
320 of changes in neuronal firing. Moreover, [although fMRI and EGR1 expression methods differ substantially](#)
321 [in the physiological events they measure, the time course for activation to be detected and the](#)
322 [wakefulness of the animals during auditory stimulation](#), both methods indicated activity in the CMM and
323 NCC is modulated by ~~the social context~~ [social-context induced song variation](#). ~~of song playback despite~~
324 ~~differences in the physiological events they measure, the time course for activation to be detected and~~
325 ~~the wakefulness of the animals during auditory stimulation~~. Thus, despite these methodological
326 differences and in line with previous observations [25], the selectivity of the regions localized using *in vivo*
327 fMRI, could be validated using the *ex vivo* technique. One substantial difference, however, is that
328 significant lateralization of FD song selectivity was apparent only in the results of the fMRI experiment.
329 For the NCC, FD selective BOLD responses were only detected in the left hemisphere. One caveat is that,
330 overall, responses to both stimuli were higher in the left than the right hemisphere. Thus, an alternative
331 possibility is that the lack of a difference in responses to FD and UD song in the right hemisphere arises
332 not because of functional lateralization but due to an overall lower level of activation. Lateralized
333 manipulations of activity in the NCC will prove interesting to understanding the degree of lateralization of
334 this region. In contrast, the overall level of activation was similar in the two hemispheres in the CMM for
335 both techniques. Consequently, the lack of selective BOLD responses in the left CMM is likely not due to
336 lower sensitivity but rather is indicative of functional lateralization. More research on the nature of
337 lateralized responses to song in the auditory forebrain and the effect of anesthesia are necessary to fully
338 understand the discrepancies in responses between the two techniques.

339 In humans there is well-established lateralization of language to the left hemisphere. However,
340 additionally, there is substantial variation in the degree and direction of lateralization for perception of
341 characteristics of speech, for example vocal prosodic features including spectral and temporal
342 characteristics that vary with emotional content [61-64]. In particular, it is hypothesized that the right
343 hemisphere may be more significant in lower-order processing of complex auditory stimuli while the left
344 hemisphere is significant for the higher-order processing of internal representations [64]. These data
345 provide an interesting parallel to the differences [we describe here](#) in hemispheric dominance between
346 the CMM (right dominant) and NCC (left dominant) in songbirds, especially given potential similarities in
347 the function and types of variation in acoustic features between FD and UD song and prosodic changes in
348 speech. Moreover, there is considerable debate as to whether hemispheric differences arise from higher-
349 order areas feeding back into auditory cortical regions (top-down influences) or whether they arise from
350 inherent, hemispheric differences in the spectrotemporal resolution in the auditory cortex (bottom-up;
351 [62]). In songbirds, a number of the inputs to the CMM and NCC show hemispheric dominance, including
352 the NCM and the MD. In the NCM, which provides input to both the CMM and NCC, the dominant
353 hemisphere appears to vary depending on the nature of the stimulus and the auditory experience of the
354 bird [65-70]. Circuit breaking experiments in songbirds may help to provide better insight into the types
355 of circuit level interactions that contribute to hemispheric differences in the processing of complex,
356 behaviorally-relevant, auditory stimuli.

357 To date, little is known about the function of regions in the caudocentral nidopallium, including the NCC,
358 beyond what has been postulated based on connectivity. However, one of the few functional studies has
359 implicated a region posterior to the NCC in male courtship behavior [71-74]. In particular, a region within
360 the central part of the caudal nidopallium (referred to as the caudal arcopallium/nidopallium, 'ANC') that
361 lies just caudal to the NCC exhibits increased 2-deoxyglucose expression following courtship behavior in
362 male zebra finches [73, 74]. Meanwhile, our data reveal that responses in the NCC are directly correlated
363 to behavioral call-back responses in female zebra finches. Further study is necessary to elucidate whether
364 the NCC and ANC represent sex-specific specializations of the caudocentral nidopallium, differentially
365 important for courtship behavior and sexual decision-making in males and females. However, our data
366 suggests that the NCC in female finches is important for evaluating and coordinating responses to socially
367 modulated acoustic signals and raises the possibility that the NCC serves as an integrative hub for sensory
368 and motor connections important in vocal communication and mate choice.

369 **ACKNOWLEDGEMENTS**

370 We thank Vivian Ng and Michele Kim for their help in collecting the behavioural data and Gaurav
371 Majumdar and Garima Yadav for their assistance in sample preparation for the TH IC. This research was
372 supported by grants from the Research Foundation – Flanders (FWO, Project No. G030213N and
373 G044311N), the Hercules Foundation (Grant No. AUHA0012), and Interuniversity Attraction Poles (IAP
374 ‘PLASTOCINE’: P7/17) to AVdL, grants from the German Research Foundation (DGN, Project No. SFB 874
375 and Gu227/16-1) to O.G, and grants from the National Sciences and Engineering Research Council (Project
376 No. RGPIN402186 and RGPIN402417 (main grant holder: Jon Sakata)) to S.C.W. L.VR and J.H are PhD
377 fellows supported by the FWO and the University of Antwerp respectively.

378 **AUTHOR CONTRIBUTIONS**

379 Conceived and designed the experiments: L.VR, S.C.W, and A.vdL; Performed the fMRI experiments: L.VR;
380 performed the behavioural and EGR1 ICC experiments: Y.C. and S.C.W.; performed the TH
381 immunostaining: K.vE and O.G; Performed final data analysis: L.VR; Advised on and contributed to data
382 analysis: J.H, G.dG, M.V and S.C.W.; Contributed reagents, materials and/or analysis tools: O.G, S.C.W, and
383 A.vdL; Contributed to data interpretation: L.VR, O.G, S.C.W and A.vdL; Wrote the paper: L.VR, O.G., S.C.W,
384 and A.vdL. All authors critically reviewed the manuscript; S.C.W and A.vdL approved the final version of
385 the manuscript.

386 **DECLARATION OF INTEREST**

387 The authors declare no competing interests.

388

389

390 **REFERENCES**

- 391 1. Darwin, C. (1871). *The descent of man, and selection in relation to sex*, (London: J. Murray).
- 392 2. Andersson, M. (1994). *Sexual Selection*, (Princeton, New Jersey: Princeton University Press).
- 393 3. Bradbury, J., and Vehrencamp, S. (1998). *Principles of animal communication*, (Sunderland: Sinauer Associates).
- 394 4. Rosenthal, G.G. (2017). *Mate Choice: The Evolution of Sexual Decision Making from Microbes to Humans*, (Princeton University Press).
- 396 5. Capranica, R.R. (1978). Auditory processing in anurans. *Fed. Proc.* *37*, 2324-2328.
- 397 6. Ryan, M. (1985). *The tungara frog: a study in sexual selection and communication*. (Chicago: Univ. Chicago Press).
- 398 7. Akre, K.L., Farris, H.E., Lea, A.M., Page, R.A., and Ryan, M.J. (2011). Signal perception in frogs and bats and the evolution of mating signals. *Science* *333*, 751-752.
- 400 8. West, M.J., and King, A.P. (1988). Female visual displays affect the development of male song in the cowbird. *Nature* *334*, 244-246.
- 401 9. King, A.P., West, M.J., and Goldstein, M.H. (2005). Non-Vocal Shaping of Avian Song Development: Parallels to Human Speech Development. *Ethology* *111*, 101-117.
- 402 10. King, A.P., and West, M.J. (1983). Epigenesis of cowbird song[mdash]A joint endeavour of males and females. *Nature* *305*, 704-706.
- 403 11. Zann, R.A. (1996). *The zebra finch: A synthesis of field and laboratory studies*, (Oxford: Oxford University Press).
- 404 12. Sossinka, R., and Böhner, J. (1980). Song types in the zebra finch (*Poephila guttata castanotis*). *Z. Tierpsychol.* *53*, 9.
- 405 13. Riebel, K. (2009). Song and Female Mate Choice in Zebra Finches: A Review. In *Advances in the Study of Behavior*, Volume Volume 40. (Academic Press), pp. 197-238.
- 406 14. Clayton, N.S. (1988). Song discrimination learning in zebra finches *Anim. Behav.* *36*, 1016-1024.
- 407 15. Miller, D.B. (1979). The acoustic basis of mate recognition by female Zebra finches (*Taeniopygia guttata*). *Anim. Behav.* *27*, 376-380.
- 408 16. Miller, D.B. (1979). Long-term recognition of father's song by female zebra finches. *Nature* *280*, 389-391.
- 409 17. Woolley, S.C., and Doupe, A.J. (2008). Social context-induced song variation affects female behavior and gene expression. *PLoS Biol.* *6*, e62.
- 410 18. Holveck, M.-J., and Riebel, K. (2007). Preferred songs predict preferred males: consistency and repeatability of zebra finch females across three test contexts. *Anim. Behav.* *74*, 297-309.
- 411 19. Chen, Y., Clark, O., and Woolley, S.C. (2017). Courtship song preferences in female zebra finches are shaped by developmental auditory experience. *Proc. R. Soc. Lond. B. Biol. Sci.* *284*.
- 412 20. Van Ruijssevelt, L., Van der Kant, A., De Groof, G., and Van der Linden, A. (2013). Current state-of-the-art of auditory functional MRI (fMRI) on zebra finches: Technique and scientific achievements. *J. Physiol. Paris* *107*, 156-169.
- 413 21. Van Ruijssevelt, L., De Groof, G., Van der Kant, A., Poirier, C., Van Audekerke, J., Verhoye, M., and Van der Linden, A. (2013). Functional magnetic resonance imaging (fMRI) with auditory stimulation in songbirds. *JoVE* *3*.
- 414 22. Voss, H.U., Tabelow, K., Polzehl, J., Tchernichovski, O., Maul, K.K., Salgado-Commissariat, D., Ballon, D., and Helekar, S.A. (2007). Functional MRI of the zebra finch brain during song stimulation suggests a lateralized response topography. *Proc. Natl. Acad. Sci. U. S. A.* *104*, 10667-10672.
- 415
- 416
- 417
- 418
- 419
- 420
- 421
- 422
- 423
- 424
- 425
- 426
- 427
- 428
- 429
- 430
- 431
- 432
- 433
- 434

- 435 23. Van Meir, V., Boumans, T., De Groof, G., Van Audekerke, J., Smolders, A., Scheunders, P., Sijbers,
436 J., Verhoye, M., Balthazart, J., and Van der Linden, A. (2005). Spatiotemporal properties of the
437 BOLD response in the songbirds' auditory circuit during a variety of listening tasks. *Neuroimage*
438 *25*, 1242-1255.
- 439 24. Boumans, T., Theunissen, F.E., Poirier, C., and Van Der Linden, A. (2007). Neural representation of
440 spectral and temporal features of song in the auditory forebrain of zebra finches as revealed by
441 functional MRI. *Eur. J. Neurosci.* *26*, 2613-2626.
- 442 25. Boumans, T., Vignal, C., Smolders, A., Sijbers, J., Verhoye, M., Van Audekerke, J., Mathevon, N.,
443 and Van der Linden, A. (2008). Functional magnetic resonance imaging in zebra finch discerns the
444 neural substrate involved in segregation of conspecific song from background noise. *J.*
445 *Neurophysiol.* *99*, 931-938.
- 446 26. Poirier, C., Verhoye, M., Boumans, T., and Van der Linden, A. (2010). Implementation of spin-echo
447 blood oxygen level-dependent (BOLD) functional MRI in birds. *NMR Biomed.* *23*, 1027-1032.
- 448 27. van der Kant, A., Derégnaucourt, S., Gahr, M., Van der Linden, A., and Poirier, C. (2013).
449 Representation of Early Sensory Experience in the Adult Auditory Midbrain: Implications for Vocal
450 Learning. *PLoS One* *8*, e61764.
- 451 28. Poirier, C., Vellema, M., Verhoye, M., Van Meir, V., Wild, J.M., Balthazart, J., and Van Der Linden,
452 A. (2008). A three-dimensional MRI atlas of the zebra finch brain in stereotaxic coordinates.
453 *Neuroimage* *41*, 1-6.
- 454 29. Karten, H.J., Brzozowska-Prechtel, A., Lovell, P.V., Tang, D.D., Mello, C.V., Wang, H., and Mitra, P.P.
455 (2013). Digital atlas of the zebra finch (*Taeniopygia guttata*) brain: a high-resolution photo atlas.
456 *J. Comp. Neurol.* *521*, 3702-3715.
- 457 30. Karino, G., George, I., Loison, L., Heyraud, C., De Groof, G., Hausberger, M., and Cousillas, H.
458 (2016). Anesthesia and brain sensory processing: impact on neuronal responses in a female
459 songbird. *Sci. Rep.* *6*, 39143.
- 460 31. Gaese, B.H., and Ostwald, J. (2001). Anesthesia Changes Frequency Tuning of Neurons in the Rat
461 Primary Auditory Cortex. *J. Neurophysiol.* *86*, 1062-1066.
- 462 32. Capsius, B., and Leppelsack, H.-J. (1996). Influence of urethane anesthesia on neural processing in
463 the auditory cortex analogue of a songbird. *Hear. Res.* *96*, 59-70.
- 464 33. Gunturkun, O. (2005). The avian 'prefrontal cortex' and cognition. *Curr. Opin. Neurobiol.* *15*, 686-
465 693.
- 466 34. Gunturkun, O., and Bugnyar, T. (2016). Cognition without Cortex. *Trends Cogn. Sci.* *20*, 291-303.
- 467 35. Waldmann, C., and Gunturkun, O. (1993). The dopaminergic innervation of the pigeon
468 caudolateral forebrain: immunocytochemical evidence for a 'prefrontal cortex' in birds? *Brain Res.*
469 *600*, 225-234.
- 470 36. Wynne, B., and Gunturkun, O. (1995). Dopaminergic innervation of the telencephalon of the
471 pigeon (*Columba livia*): a study with antibodies against tyrosine hydroxylase and dopamine. *J.*
472 *Comp. Neurol.* *357*, 446-464.
- 473 37. Bottjer, S.W., Brady, J.D., and Cribbs, B. (2000). Connections of a motor cortical region in zebra
474 finches: relation to pathways for vocal learning. *J. Comp. Neurol.* *420*, 244-260.
- 475 38. Bottjer, S.W., Alderete, T.L., and Chang, D. (2010). Conjunction of vocal production and perception
476 regulates expression of the immediate early gene ZENK in a novel cortical region of songbirds. *J.*
477 *Neurophysiol.* *103*, 1833-1842.
- 478 39. Leitner, S., Voigt, C., Metzdorf, R., and Catchpole, C.K. (2005). Immediate early gene (ZENK, Arc)
479 expression in the auditory forebrain of female canaries varies in response to male song quality. *J.*
Neurobiol. *64*, 275-284.

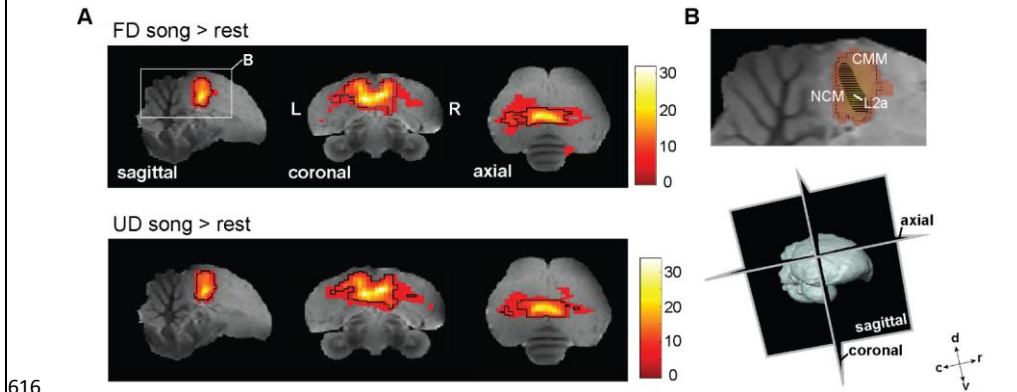
- 481 40. Gobes, S.M., Ter Haar, S.M., Vignal, C., Vergne, A.L., Mathevon, N., and Bolhuis, J.J. (2009).
482 Differential responsiveness in brain and behavior to sexually dimorphic long calls in male and
483 female zebra finches. *J. Comp. Neurol.* 516, 312-320.
- 484 41. Lampen, J., Jones, K., McAuley, J.D., Chang, S.E., and Wade, J. (2014). Arrhythmic song exposure
485 increases ZENK expression in auditory cortical areas and nucleus taeniae of the adult zebra Finch.
486 *PLoS One* 9, e108841.
- 487 42. Theunissen, F.E., and Doupe, A.J. (1998). Temporal and spectral sensitivity of complex auditory
488 neurons in the nucleus HVC of male zebra finches. *J. Neurosci.* 18, 3786-3802.
- 489 43. Woolley, S.M., Fremouw, T.E., Hsu, A., and Theunissen, F.E. (2005). Tuning for spectro-temporal
490 modulations as a mechanism for auditory discrimination of natural sounds. *Nat. Neurosci.* 8, 1371-
491 1379.
- 492 44. Woolley, S.M., and Rubel, E.W. (1999). High-frequency auditory feedback is not required for adult
493 song maintenance in Bengalese finches. *J. Neurosci.* 19, 358-371.
- 494 45. Durand, S.E., Tepper, J.M., and Cheng, M.F. (1992). The shell region of the nucleus ovoidalis: a
495 subdivision of the avian auditory thalamus. *J. Comp. Neurol.* 323, 495-518.
- 496 46. Wild, J.M., Karten, H.J., and Frost, B.J. (1993). Connections of the auditory forebrain in the pigeon
497 (*Columba livia*). *J. Comp. Neurol.* 337, 32-62.
- 498 47. Shanahan, M., Bingman, V.P., Shimizu, T., Wild, M., and Gunturkun, O. (2013). Large-scale
499 network organization in the avian forebrain: a connectivity matrix and theoretical analysis. *Front.*
500 *Comput. Neurosci.* 7, 89.
- 501 48. Oetting, S., and Bischof, H.J. (1996). Sexual Imprinting in Female Zebra Finches: Changes in
502 Preferences as an Effect of Adult Experience. *Behaviour* 133, 387-397.
- 503 49. Horn, G. (2004). Pathways of the past: the imprint of memory. *Nat. Rev. Neurosci.* 5, 108-120.
- 504 50. Thode, C., Bock, J., Braun, K., and Darlison, M.G. (2005). The chicken immediate-early gene ZENK
505 is expressed in the medio-rostral neostriatum/hyperstriatum ventrale, a brain region involved in
506 acoustic imprinting, and is up-regulated after exposure to an auditory stimulus. *Neuroscience* 130,
507 611-617.
- 508 51. Zeier, H., and Karten, H.J. (1971). The archistriatum of the pigeon: organization of afferent and
509 efferent connections. *Brain Res.* 31, 313-326.
- 510 52. Wild, J.M., Li, D., and Eagleton, C. (1997). Projections of the dorsomedial nucleus of the
511 intercollicular complex (DM) in relation to respiratory-vocal nuclei in the brainstem of pigeon
512 (*Columba livia*) and zebra finch (*Taeniopygia guttata*). *J. Comp. Neurol.* 377, 392-413.
- 513 53. Cheng, M.F., Akesson, T.R., and de Lanerolle, N.C. (1987). Retrograde HRP demonstration of
514 afferent projections to the midbrain and nest calls in the ring dove. *Brain Res. Bull.* 18, 45-48.
- 515 54. Wild, J.M., and Balthazart, J. (2013). Neural pathways mediating control of reproductive behavior
516 in male Japanese quail. *J. Comp. Neurol.* 521, 2067-2087.
- 517 55. Wild, J.M., and Botelho, J.F. (2015). Involvement of the avian song system in reproductive
518 behaviour. *Biol. Lett.* 11, 20150773.
- 519 56. Wild, J.M. (1993). The avian nucleus retroambigualis: a nucleus for breathing, singing and calling.
520 *Brain Res.* 606, 319-324.
- 521 57. Atoji, Y., and Wild, J.M. (2009). Afferent and efferent projections of the central caudal nidopallium
522 in the pigeon (*Columba livia*). *J. Comp. Neurol.* 517, 350-370.
- 523 58. Behroozi, M., Ströckens, F., Stacho, M., and Gunturkun, O. (2017). Functional connectivity of the
524 pigeon hippocampal network: An rsfMRI study. *Brain. Behav. Evol. in press.*
- 525 59. Husband, S.A., and Shimizu, T. (2011). Calcium-binding protein distributions and fiber connections
526 of the nucleus accumbens in the pigeon (*Columba livia*). *J. Comp. Neurol.* 519, 1371-1394.
- 527 60. dos Santos, T.S., Kruger, J., Melleu, F.F., Herold, C., Zilles, K., Poli, A., Gunturkun, O., and Marino-
528 Neto, J. (2015). Distribution of serotonin 5-HT1A-binding sites in the brainstem and the

- hypothalamus, and their roles in 5-HT-induced sleep and ingestive behaviors in rock pigeons (*Columba livia*). *Behav. Brain Res.* 295, 45-63.
61. Kotz, S.A., Meyer, M., and Paulmann, S. (2006). Lateralization of emotional prosody in the brain: an overview and synopsis on the impact of study design. *Prog. Brain Res.* 156, 285-294.
62. Liebenthal, E., Silbersweig, D.A., and Stern, E. (2016). The Language, Tone and Prosody of Emotions: Neural Substrates and Dynamics of Spoken-Word Emotion Perception. *Front. Neurosci.* 10, 506.
63. Wildgruber, D., Ackermann, H., Kreifelts, B., and Ethofer, T. (2006). Cerebral processing of linguistic and emotional prosody: fMRI studies. *Prog. Brain Res.* 156, 249-268.
64. Gandour, J., Tong, Y., Wong, D., Talavage, T., Dziedzic, M., Xu, Y., Li, X., and Lowe, M. (2004). Hemispheric roles in the perception of speech prosody. *Neuroimage* 23, 344-357.
65. Olson, E.M., Maeda, R.K., and Gobes, S.M. (2016). Mirrored patterns of lateralized neuronal activation reflect old and new memories in the avian auditory cortex. *Neuroscience* 330, 395-402.
66. Bell, B.A., Phan, M.L., and Vicario, D.S. (2015). Neural responses in songbird forebrain reflect learning rates, acquired salience, and stimulus novelty after auditory discrimination training. *J. Neurophysiol.* 113, 1480-1492.
67. Yang, L.M., and Vicario, D. (2014). Exposure to a novel stimulus environment alters patterns of lateralization in avian auditory cortex, Volume 285.
68. Avey, M.T., Phillmore, L.S., and MacDougall-Shackleton, S.A. (2005). Immediate early gene expression following exposure to acoustic and visual components of courtship in zebra finches. *Behav. Brain Res.* 165, 247-253.
69. Moorman, S., Gobes, S.M., Kuijpers, M., Kerkhofs, A., Zandbergen, M.A., and Bolhuis, J.J. (2012). Human-like brain hemispheric dominance in birdsong learning. *Proc. Natl. Acad. Sci. U. S. A.* 109, 12782-12787.
70. Phan, M.L., and Vicario, D.S. (2010). Hemispheric differences in processing of vocalizations depend on early experience. *Proc. Natl. Acad. Sci. U. S. A.* 107, 2301-2306.
71. Sadananda, M., and Bischof, H.J. (2002). Enhanced fos expression in the zebra finch (*Taeniopygia guttata*) brain following first courtship. *J. Comp. Neurol.* 448, 150-164.
72. Sadananda, M., Korte, S., and Bischof, H.J. (2007). Afferentation of a caudal forebrain area activated during courtship behavior: a tracing study in the zebra finch (*Taeniopygia guttata*). *Brain Res.* 1184, 108-120.
73. Bischof, H.J., and Herrmann, K. (1986). Arousal enhances [14C]2-deoxyglucose uptake in four forebrain areas of the zebra finch. *Behav. Brain Res.* 21, 215-221.
74. Bischof, H.J., and Herrmann, K. (1988). Isolation-dependent enhancement of 2-[14C]deoxyglucose uptake in the forebrain of zebra finch males. *Behav. Neural Biol.* 49, 386-397.
75. Schubloom, H.E., and Woolley, S.C. (2016). Variation in social relationships relates to song preferences and EGR1 expression in a female songbird. *Dev. Neurobiol.* 76, 1029-1040.
76. Tchernichovski, O. (1991). *Sound Analysis Pro. Version 2*, June 1991 Edition. (Boston, MA: Free Software Foundation, Inc.).
77. Tchernichovski, O., Nottebohm, F., Ho, C.E., Pesaran, B., and Mitra, P.P. (2000). A procedure for an automated measurement of song similarity. *Anim. Behav.* 59, 1167-1176.
78. Jarvis, E.D., Scharff, C., Grossman, M.R., Ramos, J.A., and Nottebohm, F. (1998). For whom the bird sings: context-dependent gene expression. *Neuron* 21, 775-788.
79. Kao, M.H., and Brainard, M.S. (2006). Lesions of an avian basal ganglia circuit prevent context-dependent changes to song variability. *J. Neurophysiol.* 96, 1441-1455.
80. Poirier, C., Boumans, T., Vellema, M., De Groof, G., Charlier, T.D., Verhoye, M., Van der Linden, A., and Balthazart, J. (2011). Own song selectivity in the songbird auditory pathway: suppression by norepinephrine. *PLoS One* 6, e20131.

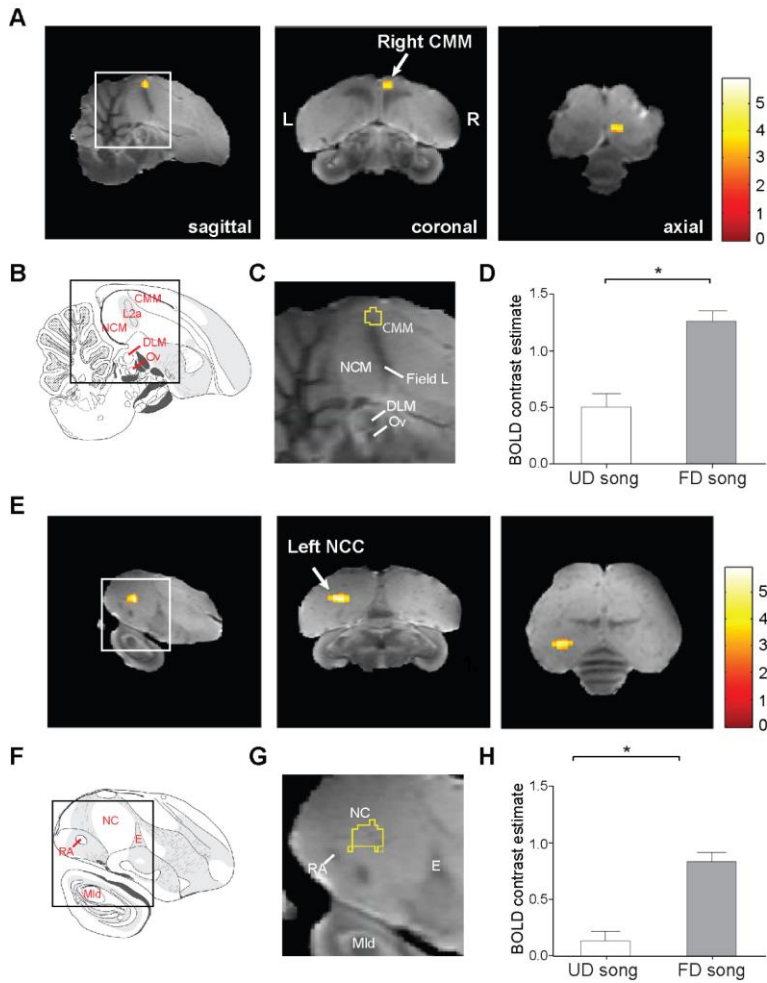
- 577 81. Poirier, C., Boumans, T., Verhoye, M., Balthazart, J., and Van der Linden, A. (2009). Own-song
578 recognition in the songbird auditory pathway: selectivity and lateralization. *J. Neurosci.* 29, 2252-
579 2258.
- 580 82. Mello, C.V., and Ribeiro, S. (1998). ZENK protein regulation by song in the brain of songbirds. *J.*
581 *Comp. Neurol.* 393, 426-438.
- 582 83. Matheson, L.E., and Sakata, J.T. (2015). Catecholaminergic contributions to vocal communication
583 signals. *Eur. J. Neurosci.* 41, 1180-1194.
- 584 84. Matheson, L.E., Sun, H., and Sakata, J.T. (2015). Forebrain circuits underlying the social
585 modulation of vocal communication signals. *Dev. Neurobiol.*
- 586 85. Bharati, I.S., and Goodson, J.L. (2006). Fos responses of dopamine neurons to sociosexual stimuli
587 in male zebra finches. *Neuroscience* 143, 661-670.
- 588 86. Stacho, M., Letzner, S., Theiss, C., Manns, M., and Gunturkun, O. (2016). A GABAergic tecto-
589 tegmento-tectal pathway in pigeons. *J. Comp. Neurol.* 524, 2886-2913.
- 590 87. Hellmann, B., and Gunturkun, O. (2001). Structural organization of parallel information processing
591 within the tectofugal visual system of the pigeon. *J. Comp. Neurol.* 429, 94-112.
- 592 88. Shu, S., Ju, G., and Fan, L. (1988). The glucose oxidase-DAB-nickel method in peroxidase
593 histochemistry of the nervous system. *Neurosci. Lett.* 85, 169-171.
- 594 89. Jiao, Y., Sun, Z., Lee, T., Fusco, F.R., Kimble, T.D., Meade, C.A., Cuthbertson, S., and Reiner, A.
595 (1999). A simple and sensitive antigen retrieval method for free-floating and slide-mounted tissue
596 sections. *J. Neurosci. Methods* 93, 149-162.
- 597 90. Bottjer, S.W. (1993). The distribution of tyrosine hydroxylase immunoreactivity in the brains of
598 male and female zebra finches. *J. Neurobiol.* 24, 51-69.
- 599 91. Sathyanesan, A., Ogura, T., and Lin, W. (2012). Automated measurement of nerve fiber density
600 using line intensity scan analysis. *J. Neurosci. Methods* 206, 165-175.
- 601 92. Rutstein, A.N., Brazill-Boast, J., and Griffith, S.C. (2007). Evaluating mate choice in the zebra finch.
602 *Anim. Behav.* 74, 1277-1284.
- 603 93. Dunning, J.L., Pant, S., Bass, A., Coburn, Z., and Prather, J.F. (2014). Mate choice in adult female
604 Bengalese finches: females express consistent preferences for individual males and prefer female-
605 directed song performances. *PLoS One* 9, e89438.
- 606 94. Cardin, J.A., and Schmidt, M.F. (2003). Song System Auditory Responses Are Stable and Highly
607 Tuned During Sedation, Rapidly Modulated and Unselective During Wakefulness, and Suppressed
608 By Arousal. *Journal of Neurophysiology* 90, 2884-2899.
- 609 95. Schumacher, J.W., Schneider, D.M., and Woolley, S.M.N. (2011). Anesthetic state modulates
610 excitability but not spectral tuning or neural discrimination in single auditory midbrain neurons.
611 *Journal of Neurophysiology* 106, 500-514.
- 612 96. Narayan, R., Graña, G., and Sen, K. (2006). Distinct Time Scales in Cortical Discrimination of Natural
613 Sounds in Songbirds. *Journal of Neurophysiology* 96, 252-258.

614

615 **MAIN-TEXT FIGURE LEGENDS**

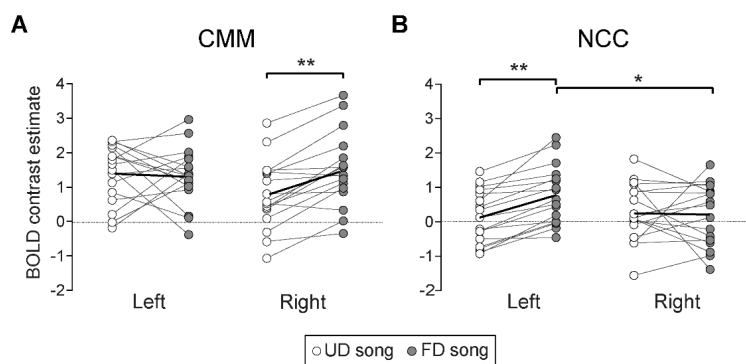


617 **Figure 1. Song playback induces robust responses throughout the auditory forebrain.** Auditory forebrain
618 activation in response to FD (top) and UD (bottom) song. (A) Statistical group maps are superimposed on
619 images from the zebra finch MRI atlas [28] Voxel T-values are color coded according to the scales on the
620 right and only voxels with T-values > 4.79 ($p < 0.0001$) are displayed. The black contours delineate voxels
621 with T-values > 7.47 ($p_{FWE} < 0.05$). (B) Inset from the sagittal view in (A) indicating the location of the
622 primary auditory subfield L2a as well as the secondary auditory regions CMM and NCM. Abbreviations:
623 (FD) female directed, (UD) undirected; (CMM) caudomedial mesopallium, (NCM) caudomedial
624 nidopallium; (c) caudal, (d) dorsal, (L) left, (R) right, (r) rostral, (v) ventral. (n=17)

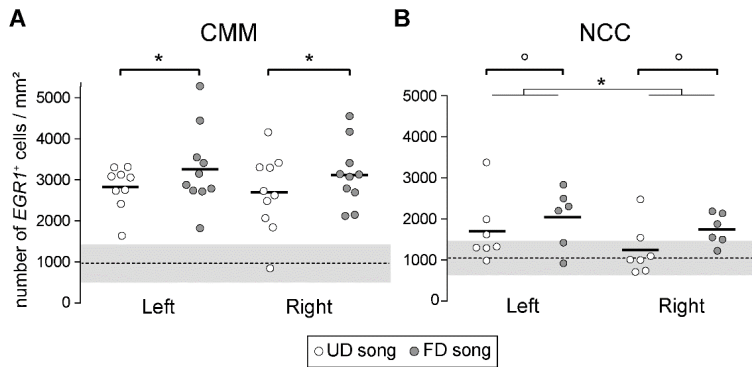


625
 626 **Figure 2. fMRI reveals two regions that are selective for FD song.** Significantly higher BOLD responses
 627 induced by FD song playback compared to UD song playback were identified in the caudomedial
 628 mesopallium (CMM; A-D) and the caudocentral nidopallium (NCC; E-H). (A, E) Three views (sagittal [left],
 629 coronal [middle], and axial [right]) of the respective clusters in the CMM (A) and the NCC (B) with
 630 significantly higher BOLD responses induced by FD song playback relative to UD song playback. Images are
 631 statistical maps superimposed on zebra finch MRI atlas images [28] T values are color coded according to
 632 the scale (right) and all cluster voxels with t-values > 2.60 (p<0.01) are displayed. The coronal (middle)

633 panel highlights the substantial lateralization of the BOLD response. (B, F) Line-drawings of sagittal
 634 sections from the zebra finch histological atlas browser (Oregon Health & Science University, Portland, OR
 635 97239; <http://www.zebrafinchatlas.org>; [29] (C, G) Detailed view of the exact locations of the clusters
 636 within the CMM and the NCC (magnification of the region outlined in black in respectively B and F). (D, H)
 637 The relative BOLD response amplitude (vs. rest) in the identified cluster was significantly greater in
 638 response to FD than UD song. The values (\pm SEM) are from the voxel with the maximum T value (FD vs.
 639 UD) and the zero level corresponds to the estimated mean during rest periods. Abbreviations: (FD) female
 640 directed, (UD) undirected; (CMM) caudomedial mesopallium, (DLM) medial dorsolateral nucleus of the
 641 anterior thalamus, (E) entopallium, (Mld) dorsal part of the later mesencephalic nucleus, (NCM)
 642 caudomedial nidopallium, (NCC) caudocentral nidopallium, (Ov) nucleus ovoidalis, (RA) robust nucleus of
 643 the arcopallium. (* $p_{\text{uncorr}} < 0.001$; $n=17$).

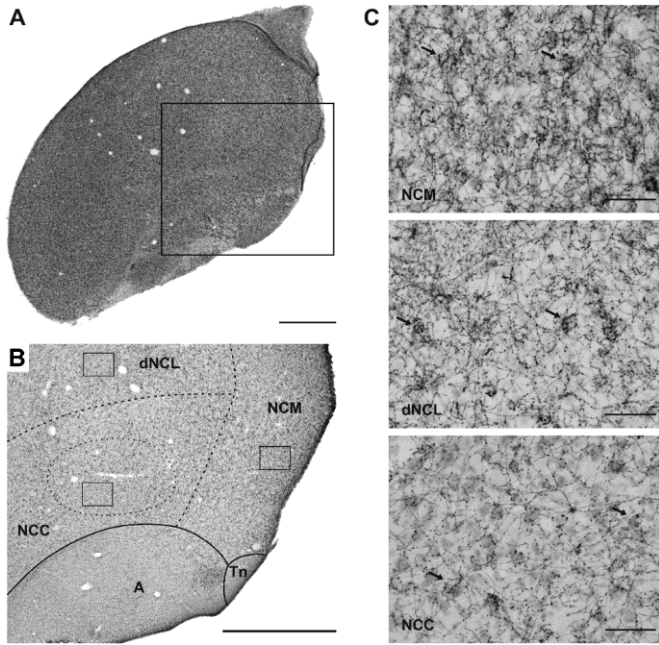


644
 645 **Figure 3. BOLD response to FD and UD song in female zebra finches is highly lateralized.** Average relative
 646 BOLD response amplitude (vs. rest) in the CMM (A) and the NCC (B) elicited by FD and UD song across
 647 voxels within the identified FD song selective clusters (right CMM and left NCC) and their mirrored
 648 counterparts. The zero level corresponds to the estimated mean during rest periods. The bold line
 649 corresponds to the group mean and points are responses for individual females. Abbreviations: (FD)
 650 female directed, (UD) undirected; (CMM) caudomedial mesopallium, (NCC) caudocentral nidopallium.
 651 (* $p < 0.05$; ** $p < 0.001$; $n=17$). See also Figure S1.



652

653 **Figure 4. FD song elicits greater EGR1 expression than UD song in both the CMM and NCC.** The number
 654 of EGR1+ neurons per square millimeter is significantly higher following FD song playback (green) than
 655 following UD song playback (blue) in the CMM (A) and the NCC (B). Points are individual females (see
 656 methods for more details on the sample sizes), dashed lines ± shaded areas represent the
 657 mean ± standard deviation of the silence controls. Colored horizontal bars represent the group mean.
 658 Abbreviations: (FD) female directed, (UD) undirected; (CMM) caudomedial mesopallium, (NCC)
 659 caudocentral nidopallium. (*p<0.05) See also Figure S2.

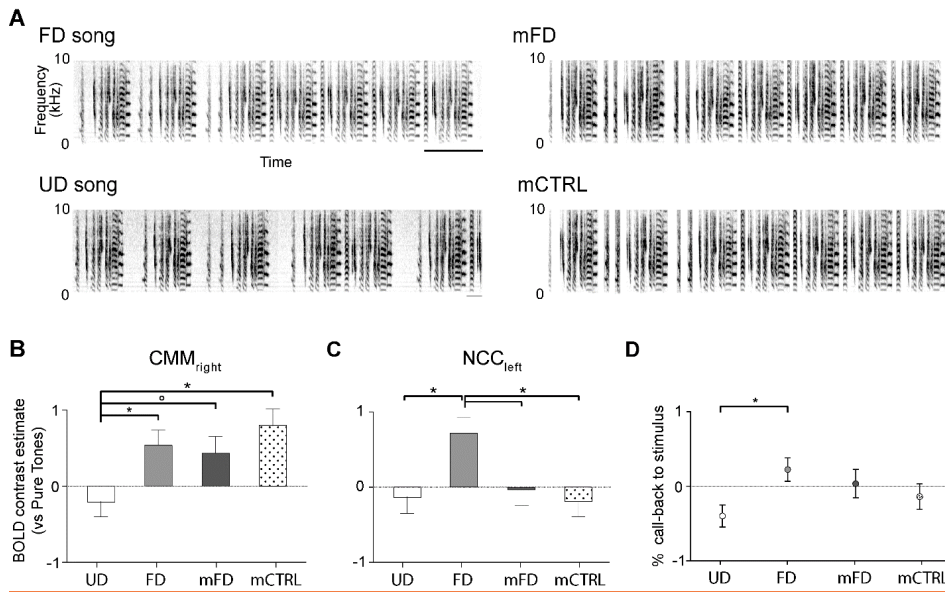


660

661 **Figure 5. Differences in TH⁺ fiber and basket densities indicate subdivisions of the caudal nidopallium.**

662 TH density was measured within the NC at the level of the FD selective NCC area. (A) Nissl stained overview
 663 image illustrating the coronal sections of interest (retrieved from the digital zebra finch brain atlas:
 664 <http://zebrafinch.brainarchitecture.org>; [29]). (B) Magnification (black square in (A)) of a representative
 665 TH stained section. Solid lines indicate known boundaries, dashed lines indicate putative region
 666 boundaries based on TH densities. Squares are the locations where TH⁺ fiber density and number of
 667 baskets were quantified. Differences in fiber density and morphology of baskets (black arrows, C) allow
 668 for an approximation of the borders of the NCM, NCL, and NCC (B). NCM can be characterized by dense
 669 innervation and a large number of highly innervated baskets (C, top), and extends approximately 1 mm
 670 from the midline. In contrast, dNCL shows fewer baskets and is moderately innervated by TH⁺ fibers (C,
 671 middle). The NCC contains very few baskets, and a low number of TH⁺ fibers. The fMRI signal of the FD
 672 song selective region is indicated by the dashed circles in (B), located within the NCC. Abbreviations: (A)
 673 arcopallium, (NCM) caudomedial nidopallium, (NCC) caudocentral nidopallium, (dNCL) dorsal caudolateral
 674 nidopallium, (Tn) nucleus taeniae. Scale bar = 1000 μm in A, B, and 50 μm in C.

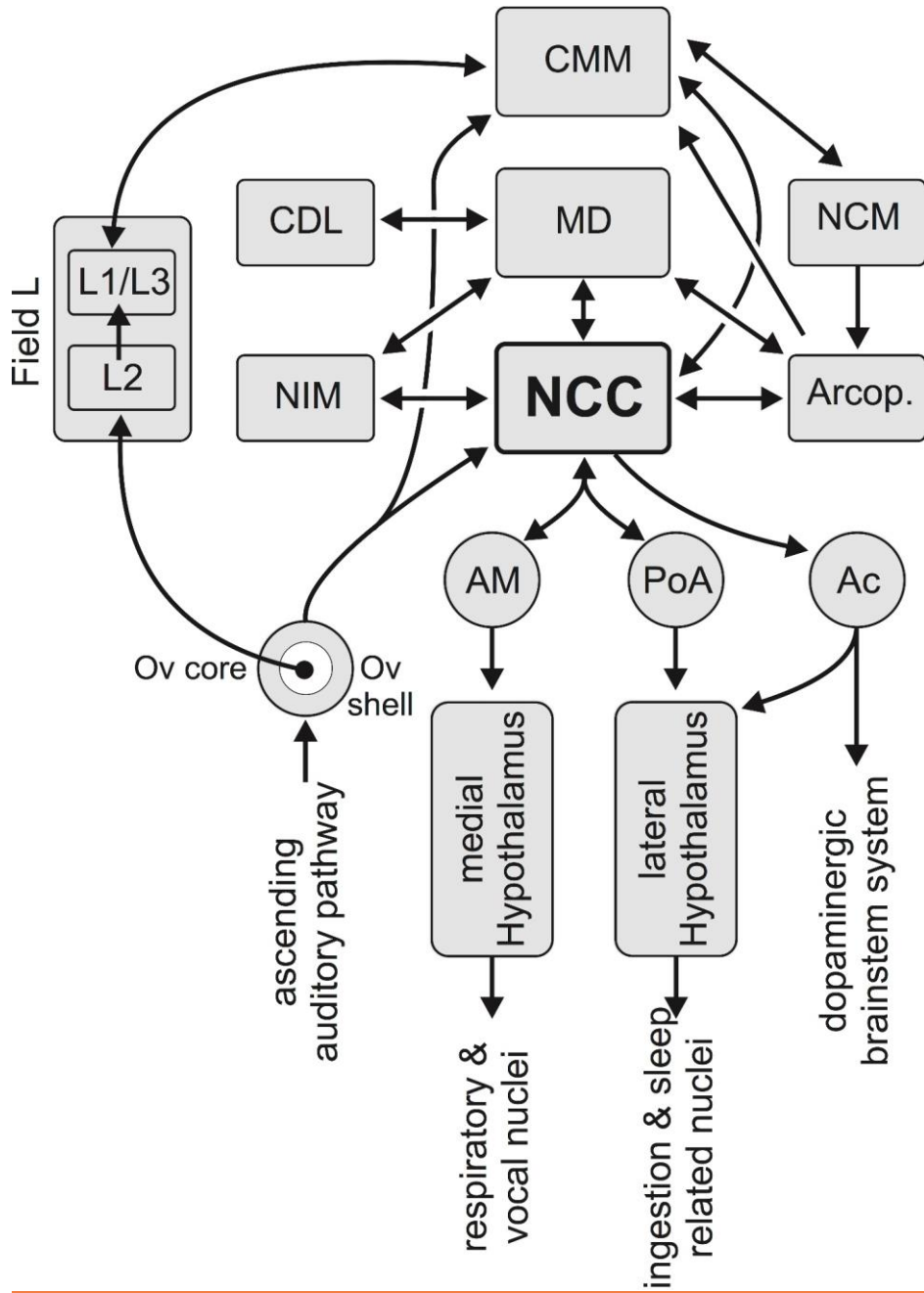
675



676

677 **Figure 6. Responses to acoustically modified versions of FD songs reveal functional differences between**
 678 **the CMM and the NCC.** (A) Representative sound spectrograms for each stimulus type (excerpts from
 679 original 16-s long stimuli). Scale bar = 1 s. (B/C) The average relative response amplitude (\pm SEM) of neural
 680 activations elicited by the different stimuli in the right CMM (B) and left NCC (C) (values from the voxel
 681 with the maximum T value for the main effect stimulus). The zero level corresponds to the estimated
 682 mean BOLD response relative to pure tones ($^*P_{FWE} < 0.1$; $^*P_{FWE} < 0.05$; $n=16$). (D) Percent change in calling
 683 (relative to the pre-stimulus period) in response to UD song, FD song, mFD song and mCTRL song. Mean
 684 \pm SEM ($^*p < 0.05$; $n=13$). Abbreviations: (FD) female directed song, (mFD) manipulated female directed
 685 song, (mCTRL) song stimulus controlling for manipulation, (UD) undirected song. See also figure S3.

686



688 **Figure 7. Suggested overview of NCC connectivity related to FD song processing and courtship behavior.**

689 The caudocentral nidopallium (NCC) receives auditory input via both the shell of the nucleus ovoidalis (Ov
690 shell) and, via the multimodal arcopallium, from the caudomedial nidopallium (NCM) [45, 47, 56]. It has
691 also reciprocal connections with the intermediate medial nidopallium (NIM) that is a part of a frontal
692 medial region for filial imprinting based on visual and auditory stimuli [49, 50]. In addition, the NCC has
693 reciprocal connections with the limbic dorsomedial mesopallium (MD) that integrates various sensory
694 streams and communicates via the dorsolateral corticoid area (CDL) with the hippocampus [57, 58]. The
695 NCC has three important down sweeping projections. One reaches via nucleus accumbens (Ac) the cell
696 groups of possibly dopaminergic nature in the midbrain [57, 59]. Thus, the NCC can modify the avian
697 reward circuit. The other descending pathways from the NCC control hypothalamic subnuclei via
698 descending projections to the posterior nucleus of the pallial amygdala (PoA) and the medial arcopallium
699 (AM). The PoA projects to areas of the lateral hypothalamus [51] that participate in various avian
700 physiological regulatory circuits controlling sleep and ingestive behavior [60]. Other descending
701 projections of the NCC run via the Ac to the cell groups of possibly dopaminergic nature in the midbrain
702 [57, 59] and via the AM to the posterior medial hypothalamus [51]. The medial hypothalamus projects to
703 multiple downstream structures like the dorsomedial nucleus of the midbrain (DM) that has descending
704 projections to brainstem respiratory and vocal nuclei [52]. List of abbreviations: (Ac) nucleus accumbens,
705 (AM) medial arcopallium, (Acrop.) arcopallium, (CDL) dorsolateral corticoid area, (CMM) caudomedial
706 mesopallium, (DM) dorsomedial nucleus of the midbrain, (MD) dorsal mesopallium, (NCC) caudocentral
707 nidopallium, (NCM) caudomedial nidopallium, (NIM) intermediate medial nidopallium, (Ov shell) shell of
708 the nucleus ovoidalis, (PoA) posterior nucleus of the pallial amygdala.

709

710 STAR METHODS

711 Contact for reagent and resource sharing

712 Further information and requests for resources and reagents should be directed to and will be fulfilled by
713 the Lead Contact, Annemie Van der Linden (Annemie.vanderlinden@uantwerp.be).

714 Experimental Model and Subject details

715 We used adult zebra finches (*Taeniopygia Guttata*, > 90 days old) which were either purchased from
716 registered breeders ([Exotic Wings and Pet Things, St. Clements, Ontario, Canada; LISBETH??](#)) or bred at
717 the local animal facility ([McGill University, Montreal, QC, Canada; Bio-Imaging lab, University of Antwerp,
718 Antwerp, Belgium](#); See Table S1 for an overview of the sample sizes per experiment). The fMRI
719 experiments were performed at the Bio-Imaging lab, University of Antwerp (Belgium) where the birds
720 were housed in large aviaries under a 12 hour light/dark cycle with access to food and water *ad libitum*.
721 The birds for the TH immunostaining were also raised in these conditions before sacrifice. The behavioral
722 experiments and the ICC analysis of EGR1 expression were performed at the Department of Biology,
723 McGill University (Canada) ~~in~~ on a separate group of birds which were ~~kept-housed~~ in single-sex group
724 cages (43 x 43 x 43 cm; <10 birds/cage) prior to testing. Birds were maintained on a 14 hour light/10 hour
725 dark photoperiod and provided with food and water *ad libitum* throughout the experiments. All
726 procedures were approved by either the University of Antwerp ethical committee (License number: 2012-
727 43) in agreement with the Belgian laws on the protection and welfare of animals (fMRI and TH ICC
728 experiments) or the McGill University Animal Care and Use Committee and in accordance with the
729 guidelines of the Canadian Council on Animal Care (behavior and EGR1 ICC).

730 Method Details

731 Auditory Stimuli

732 Song recordings

733 Stimuli were FD and UD song from five different males ('stimulus males') that were unfamiliar and
734 unrelated to the experimental females. Songs were recorded as previously described [17, 75]. Briefly,
735 males were housed individually in a cage inside a sound-attenuating chamber ('soundbox'; [TRA Acoustics](#),

736 [Cornwall, Ontario](#) containing a microphone ([Countryman Associates, California](#)) and a video camera
737 ([PalmVid, Colorado](#)). Vocalizations were recorded using a custom written sound-activated recording
738 system (44.1 kHz) or Sound Analysis Pro (SAP; [76, 77]) To collect FD song, we placed a cage containing a
739 muted female next to the male's cage in the soundbox and monitored the male's behavior on a video
740 monitor. During courtship song performance, males orient toward the female, fluff the body feathers
741 while flattening feathers on top of the head, hop, dance, and beak wipe [11, 17, 78, 79].). Only songs
742 where males performed at least two of the above courtship components were considered to be FD songs.
743 Males performed one to two bouts of song for each female presentation. After removing the female, we
744 waited up to 10 minutes before reintroducing the female in order to collect interleaved bouts of UD song.
745 We also recorded an additional one hour of UD song before the first and after the last female presentation
746 on each recording day. Males were recorded in the morning and were recorded over multiple days in
747 order to ensure a sufficient number of FD song bouts to use for stimuli.

748 Muting was performed by placing a small piece of plastic tubing inside the bronchii as described in [17].
749 Briefly, following anesthesia (~~equithesin~~ [Equithesin](#) 3.0-4.0 µg/g) we made small incisions in the skin and
750 air sac to expose the syrinx. We then made an incision along the midline of the syrinx and placed a small
751 piece of plastic tubing into each bronchia. The incision in the syrinx was closed using Nexaband (Abbott
752 Animal Health) and the skin incision was closed with suture. The females that were used to elicit FD song
753 for the recordings were not included in the remaining experiments.

754 Stimulus design

755 ~~[17]~~[17]

756 Stimuli used in the fMRI ON-OFF block paradigm had particular requirements, and we generated
757 additional, fMRI specific stimulus sets for three different males. Each set consisted of four stimulus types:
758 unmanipulated FD song, unmanipulated UD song, manipulated FD song (mFD) and a control song
759 manipulation (mCTRL; Figure 6A). For each stimulus type, we generated five to seven different examples.
760 The presentation of stimuli for fMRI in an ON-OFF block paradigm required that all stimuli be 16 seconds
761 long with minimal silence between motifs. To achieve this, we concatenated together multiple song bouts
762 from a single male to create each 16 second-long stimulus.

763 The manipulated stimuli switched the temporal and spectral characteristics between the FD and UD songs.
764 Specifically, for one type (mFD), UD song syllables (spectral characteristics) were presented with the
765 temporal characteristics (intersyllable and intermotif intervals) of FD song. To generate the manipulated

766 stimuli, we determined syllable boundaries for all syllables in all of the recordings that we had for each
767 bird using an automated, amplitude-based segmentation algorithm in Matlab. Each syllable was then
768 given an identifying label and we measured the duration of all syllables and gaps in the FD and UD songs
769 that we recorded from a single male. We also measured the specific durations of syllables and gaps in
770 each of the concatenated FD and UD stimuli described above. To create the mFD stimuli, we replaced
771 each syllable in each concatenated FD song with a UD syllable of the same syllable type. We selected UD
772 syllables with durations that exactly matched the durations of the specific syllable in the concatenated FD
773 song they replaced. For the inter-syllable intervals, we used the measurements of the inter-syllable
774 intervals in the concatenated stimuli to create silent gaps between syllables. Thus, the manipulated stimuli
775 replicate the syllable and interval durations of each concatenated stimulus. To control for subtle effects
776 resulting from the cutting and pasting of syllables, including increased amplitude contrast at syllable
777 onsets and offsets, we created modified control stimuli (mCTRL) that contained FD song syllables. For the
778 mCTRL we selected FD syllables with durations that exactly matched the durations of the specific syllables
779 in the concatenated FD song that they replaced. None of the syllable renditions appear more than once
780 in the stimulus sets. All manipulations were performed using custom written Matlab routines ([Mathworks,
781 Natick, MA](#)). The same FD, UD, mFD and mCTRL stimuli that were used for the fMRI stimuli were also used
782 for the behavior tests.

783 For the fMRI experiment, we also created additional artificial stimuli (16 seconds) consisting of pure tones
784 at different frequencies between 1 and 7 kHz with durations of 0.7 seconds interleaved with silence
785 periods of 0.1 to 0.2 seconds. The artificial frequency dependent increase of sound intensity by the
786 scanning setup was controlled by applying an equalizer to the stimuli upon presentation in the fMRI
787 experiment [21]. Behavioral experiments were performed using the stimuli generated for the fMRI ON-
788 OFF block paradigm.

789 For the fMRI experiment, we also created additional artificial stimuli (16 seconds) consisting of pure tones
790 at different frequencies between 1 and 7 kHz with durations of 0.7 seconds interleaved with silence
791 periods of 0.1 to 0.2 seconds. The artificial frequency dependent increase of sound intensity by the
792 scanning setup was controlled by applying an equalizer to the stimuli upon presentation in the fMRI
793 experiment [21]. Behavioral experiments were performed using the stimuli generated for the fMRI ON-
794 OFF block paradigm.

795 **Functional MRI**

796 Data acquisition

797 We imaged 19 adult females on a horizontal MR system (Pharmascan 70/16 US, Bruker Biospin, Germany)
798 with a magnetic field strength of 7 Tesla following established protocols [21]. More specifically, first, the
799 birds were anaesthetized with isoflurane (IsoFlo®, Abbott, Illinois, USA; induction: 3.0%; maintenance:
800 1.2%) in a mixture of oxygen and nitrogen (at flow rates of 100 and 200 cm³/min, respectively) delivered
801 through a beak mask fixed to the MRI scanner bed. Second, we acquired Turbo RARE T₂-weighted pilot
802 scans along three orthogonal directions to inform on the birds' position in the MRI scanner. Based on
803 these scans, we made sure all birds were positioned similarly (relative to the center of the scanner) for all
804 imaging sessions. Third, we acquired two time series of 298 T₂-weighted rapid acquisition relaxation-
805 enhanced (RARE) volumes for each bird with the following parameters: TE_{eff}/TR: 60/200 ms; matrix: 64x32
806 zero-filled to 64x64; slice number: 15; spatial resolution: (0.25x0.50x0.75)mm³ zero-filled to
807 (0.25x0.25x0.75)mm³; interslice gap: 0.05 mm; FOV: (16x16x12)mm³ (encapsulating the entire brain);
808 orientation: sagittal; RARE factor: 8; scan duration: 40 min. In between the two fMRI time series, we
809 obtained a 3-dimensional T2-weighted anatomical RARE scan with the following settings: TE 11 ms (TE_{eff}
810 44 ms), TR 3000 ms, RARE factor 8, FOV (16 x 14 x 14) mm³, matrix (256 x 92 x 64), spatial resolution (0.06
811 x 0.15 x 0.22) mm³ zero-filled to (0.06 x 0.05 x 0.05) mm³, scan duration 35 min. The 3-dimensional T2-
812 weighted RARE scan was acquired in the same orientation as the fMRI scans to facilitate later spatial
813 registration of the fMRI.

814 Auditory stimulation was delivered at 70dB through dynamic loudspeakers (Visation, Germany; magnets
815 removed), placed at each side of the bird's head. We presented females with one of four stimulus sets
816 over two testing sessions, with one session for non-manipulated (FD song, UD song) stimuli and one for
817 manipulated (mFD, mCTRL) stimuli. Besides these biologically relevant or modified sounds, we included a
818 set of reference stimuli in the form of pure tones in each session to enable comparison of stimuli across
819 sessions (e.g. FD/PT versus mDF/PT). We presented the three different stimulus types randomly in each
820 session in an ON/OFF blocked design where 16 seconds of stimulation (ON periods) and 16 seconds of rest
821 (OFF period) were alternated. The presentation order of the three stimulus types during the fMRI
822 acquisition was randomized. In addition, for the FD and UD song stimuli the presentation of the different
823 renditions of song was randomized over the stimulation blocks for the particular stimulus type. A session
824 consisted of 72 ON blocks (24 per stimulus type) and 72 OFF blocks. During each block, we acquired two
825 fMRI scans resulting in 48 time-series per stimulus type and per subject. The two fMRI sessions were

826 separated by 40 minutes (during which the 3-dimensional T2-weighted RARE scan was acquired) and the
827 order of manipulated and unmanipulated stimulus sets was randomized across birds.

828 Throughout the entire imaging protocol, the physiological condition of the animals was continuously
829 monitored by means of a pressure sensitive pad to detect the breathing rate, and a cloacal thermistor
830 probe to measure body temperature (MR-compatible Small Animal Monitoring and Gating system, SA
831 Instruments, Inc.). The latter was connected to a tightly controlled warm air feedback system to maintain
832 the birds' body temperature within narrow physiological ranges (40.0 ± 0.2) °C. All zebra finches recovered
833 uneventfully within a few minutes after the experiment.

834 Data quality assessment

835 We applied the following inclusion criteria for the fMRI time series: (1) limited head motion (< 0.5 mm
836 translation in either of 3 directions), and (2) detection of positive BOLD response in the primary auditory
837 region Field L. In the event that one of these criteria was not met, we repeated the fMRI experiment for
838 that particular individual using stimuli from a different male to ensure unfamiliarity of the presented
839 sounds during scanning. Doing so, a final success rate of more than 80% was reached, which is in line with
840 previous fMRI experiments in zebra finches [26, 80, 81].

841 Data processing

842 We performed both data preprocessing and voxel-based analysis using the Statistical Parametric Mapping
843 toolbox (SPM12, Wellcome Trust Centre for Neuroimaging, London, UK; <http://www.fil.ion.ucl.ac.uk/spm>)
844 as described in [21] with some adaptations. First, we realigned each fMRI scan time series (correct for
845 translation and rotation of the bird's head during scanning) and co-registered them to their corresponding
846 3D RARE acquired during the same imaging session using mutual information as similarity metric. Second,
847 we masked the 3D RARE scan to exclude non-brain tissue. This step appeared necessary to facilitate
848 subsequent spatial normalization steps. Third, we spatially normalized all 3D RARE images to the high-
849 resolution zebra finch MRI atlas [28] using a global 12-parameter affine transformation followed by
850 nonlinear deformations. The spatial correspondence between each individual scan and the ex vivo zebra
851 finch MRI atlas was inspected visually. In case the spatial transformation did not reach satisfactory
852 standards, the procedure was repeated until successful. Fourth, we [up-sampled the fMRI data to a final](#)
853 [resolution of \(0.125 x 0.125 x 0.400\) mm³ \[27\] and](#) applied the spatial transformation parameters
854 estimated during the previous step to the co-registered fMRI scan time series. This way all fMRI data were

855 transformed into the zebra finch MRI atlas space. Fifth, we smoothed the fMRI images in-plane using a
856 Gaussian kernel of 0.5 mm full width at half maximum (FWHM).

857 We applied a high pass filter (352 seconds cutoff period) to the data to remove low frequency drifts in the
858 BOLD signal. For each subject, we subsequently modeled the BOLD responses as a box-car function
859 convolved with a canonical hemodynamic response function within the framework of the general linear
860 model to analyze brain activation differences related to the onset of the different stimuli. We included
861 the six estimated movement parameters derived from the realignment corrections as regressors in the
862 model to account for the residual effect of head motion. After the estimation of the GLM parameters (β),
863 we calculated different t-contrast images (containing weighted parameter estimates) for different
864 comparisons including FD song, UD song, mFD and mCTRL > rest and > pure tones. These single subject
865 contrast maps were subsequently entered into appropriate statistical designs for group analysis.

866 The clusters in which a significant selectivity for FD song was found in the voxel-based group analysis (see
867 Results) were used as regions of interest (ROIs) in the subsequent ROI based analysis. To compare
868 responses in the left and right hemisphere, the ROIs identified in one hemisphere were mirrored over the
869 midline to obtain an identical ROI in the opposite hemisphere. From the single subject t-contrast maps for
870 FD song > rest and UD song > rest, we subsequently calculated the average fMRI signal over the contiguous
871 voxels in each ROI.

872 **EGR1 expression**

873 Adult females (n=24) that had not been exposed to fMRI imaging or behavior tests were placed
874 individually in sound-attenuating chambers for at least 24 hours prior to experimentation. The morning
875 of the experiment, we turned lights off at least 2 hours before initiating 30 minutes of song playback of
876 either FD or UD song from a single male [through a speaker \(Avantone, New York\)](#). We played back five to
877 seven FD or UD stimuli from a single male at 70 dB in random order with each stimulus separated by one
878 second. As with scanning during fMRI, we performed playback in the dark to minimize female calling and
879 ensure responses were only to auditory cues that occurred during the stimulation period. Females who
880 were not exposed to song playback but were otherwise treated identically to birds receiving playback,
881 were used as silence controls. After song playback, we kept females in the dark, undisturbed, for 45
882 minutes to allow for protein translation [17, 82]. Subjects were then deeply anaesthetized with isoflurane
883 vapor and transcardially perfused with 25 mL heparinized saline (100 IU/100mL) followed by 150 mL of
884 4% paraformaldehyde (pH 7.4). Brains were collected and post-fixed for 4 hours, then cryoprotected in
885 30% sucrose. We cut 40 μ m sagittal sections from the left and right hemispheres on a freezing microtome

886 (Leica Biosystems, Wetzlar, Germany) and stored these in 0.025M phosphate-buffered saline (PBS) with
887 sodium azide at 4°C.

888 For the analysis of the expression of EGR1, we performed ICC in ten batches, each of which contained
889 every third section from one bird that heard FD song and one that heard UD song. Both song-exposed
890 birds in the batch heard songs from the same stimulus male. Four batches also included a silence control.
891 We followed standard ICC procedures that have been described elsewhere [75, 83-85]. Briefly, brain
892 sections were rinsed (3 X 10-min) in 0.025M PBS then incubated in 5% donkey serum and 0.3% Triton-X.
893 Following additional rinses (3X10 min) sections were incubated for 48-h at 4°C in rabbit anti-EGR1 (1:1000
894 dilution; Santa Cruz Biotechnology, Santa Cruz, CA, USA) and either sheep anti-tyrosine hydroxylase (TH;
895 n=7 batches; 1:1000 dilution; Cat# NB300-110, Novus Biologicals, Littleton, CO, USA) or mouse anti-NeuN
896 (n=3 batches; 'Neuronal Nuclei'; 1 : 1000 dilution; Cat# MAB377; EMD Millipore, Billerica, MA, USA).
897 Sections were then washed (3 X 10-min) and incubated for 2-h at room temperature in donkey anti-rabbit
898 secondary antibody conjugated to Alexa Fluor 594 (for EGR1; 5µl/ml; Life Sciences, Burlington, ON,
899 Canada) and either donkey anti-sheep (for TH) or donkey anti-mouse (for NeuN) secondary antibody
900 conjugated Alexa Fluor 488 (3µl/ml; Life Sciences). Following another wash (3 X 10-min), sections were
901 mounted and cover-slipped (ProLong Gold Antifade Reagent, Life Sciences) on chromium-aluminium
902 subbed slides.

903 We imaged EGR1-immunoreactive (EGR1-ir) neurons in the two regions found to be selective for FD song
904 in the fMRI experiment, the CMM and the NCC. For the CMM, we sampled in the most caudal area dorsal
905 to the mesopallial lamina and ventral to the lateral ventricle [17]. The results for this region served as a
906 control group in a previously published study [19]. For the identified region in the NC, sampling was guided
907 by the MRI results. Lateral sections from batch 1-3 were not available, so NC analysis was only performed
908 in batches 4-10. Damaged sections were excluded and if fewer than two sections remained for a given
909 hemisphere of a specific region, the result for that hemisphere was left out of the statistical analysis (n=1
910 (UD) for right CMM; n=1 (FD) for left NCC; n=1 for right NCC). For each region, monochrome
911 photomicrographs of EGR1 expression were taken in each hemisphere with a 40X objective using a Zeiss
912 Axio Imager upright microscope and an AxioCam MRm Zeiss camera (Carl Zeiss, Jena, Germany). Using Fiji
913 imaging software (NIH), EGR1-ir neurons were manually counted in a (225 X 170) µm² window on multiple
914 sections (see Figure S2 for representative images). Imaging and cell counts were performed by a
915 researcher blind to the playback condition of the individual bird. Fiji was used to ensure consistency of

916 thresholds for determining labeled neurons across sections within an individual bird as well as between
917 birds.

918

919 **TH expression**

920 Two females and two males were deeply anaesthetized with sodium pentobarbital (Doléthel, 0.25 g/kg,
921 i.p.) and transcardially perfused with ice-cold saline (pH 7.4) followed by 4% paraformaldehyde (pH 7.4).
922 Brains were collected and post-fixed overnight (<15 hours) then cryoprotected in 20% sucrose (4°C, 10
923 hours) followed by 30% sucrose. We cut 40µm coronal sections in 10 parallel series (Leica Microsystems,
924 Wetzlar, Germany) and stored these in 0.1% sodium azide in PBS at 4°C. As previously described [86], the
925 immunochemical detection of TH took place in one series of free-floating sections with the avidin/biotin-
926 technique [87] visualized by 3,3'-diaminobenzidine (DAB) with cobalt-nickel enhancement [88]. The
927 protocol was refined with the addition of a defixation step using heat-induced-epitope-retrieval [89], and
928 an optimal antibody concentration as established in different avian species (von Eugen, unpublished).
929 More specifically, the protocol consisted of the following steps which were all performed at room
930 temperature, unless otherwise stated. Incubation was done using a slow 7° rotator and washes (3 X 10
931 min) in 0.12 M PBS were done on a slow 5° rotator. After an initial washing step of the slices, we performed
932 heat-induced epitope-retrieval. One series of free-floating sections were placed in 10 mM preheated
933 sodium citrate (pH 8.5-9.0) and maintained at 80°C for 30 minutes. The slides were then washed and
934 incubated in 0.6% H₂O₂ in 0.12 M PBS to deactivate endogenous peroxidase. After another washing step,
935 sections were incubated for 30 minutes in 10% normal-horse-serum (NHS) in 0.3% Triton-X-100 in 0.12 M
936 PBS (PBST). Next, slides were washed and incubated in the primary antibody (monoclonal mouse anti-TH
937 (MAB5280, MerckMillipore, Darmstadt, Germany), 1:500 in PBST) for 70 hours at 4°C. Following
938 incubation, slides were washed again and incubated in the secondary antibody (biotinylated horse anti-
939 mouse IgG (Vectastain Elite ABC Kit, Horse IgG, Vector), 1:500 in PBST) for 1 hour. After another washing
940 step, sections were incubated in avidin/biotin complex (Vectastain Elite ABD Kit, 1:100 in PBST) for 1 hour.
941 The bound complex was visualized with 3,3'-diaminobenzidine (DAB; Sigma-Aldrich) with cobalt-nickel
942 enhancement. After staining, sections were mounted on gelatin-covered glass slides, dried, dehydrated
943 and coverslipped using DePex (Sigma-Aldrich). Subsequently, we selected the left and right hemisphere
944 of the eight most caudal slices based on previous descriptions of TH distribution in the zebra finch [90]
945 and on the location of the NC sub-region from the fMRI analysis (see fMRI results). Pictures were taken
946 using a Zeiss Axio Imager M1 Microscope (Carl Zeiss MicroImaging, Gottingen, Germany) with the 20x

947 objective as well as a 40x objective within regions of interest for a closer examination of basket
948 morphology.

949 We assessed TH fiber density using a custom written automatic program (Sepideh Tabrik, research
950 assistant at Ruhr-Universität Bochum, Germany). Following [91], the program employs a Hessian based
951 curvilinear feature extraction in ImageJ (version 1.48, U.S. National Institutes of Health, Bethesda,
952 Maryland, USA). Hessian image filters are most suitable to extract curvilinear structures, and thus fibers.
953 Next, we executed a baseline adjustment and peak detection on the filtered images in MATLAB (version
954 R2016a, MathWorks, Natick, MA, USA). The baseline adjustment increases the signal to noise ratio
955 within the image, and the peak detection quantifies the number of high-intensity pixels above a specified
956 threshold, representing the stained fibers, on a projected (grid)-line. The threshold was determined from
957 an unstained area within the brain slide. The program returns an approximation of TH⁺-fiber density per
958 150 μm² over the whole brain slice. These results allowed for a qualitative analysis of the trajectory of
959 fiber density differences throughout the caudal telencephalon of two females, which we verified with data
960 from two males.

961 **Call-back behavior**

962 We assessed female responses to FD and UD songs using a call-back assay [92, 93]. At least 24h prior to
963 testing, females were moved into a sound-attenuating chamber equipped with a microphone, a video
964 camera and a speaker (~~Avantone, New York~~). We performed the assays between 9am and 2pm over the
965 course of one day. The call-back assay for each stimulus consisted of a 15-minute silent period ('pre-
966 stimulus period') followed by five minutes of stimulus playback and then another 10-minute period of
967 silence ('stimulus period'). For each five-minute block of song playback, multiple renditions of FD and UD
968 song from a single male were played through a speaker in pseudorandom order using custom written
969 Matlab routines (~~Matlab, MathWorks, Natick, MA~~). A one-second interval was included between each
970 rendition resulting in a total duration of song played within the stimulus period of 4.19 ± 0.01 minutes.
971 Thirteen females were tested with FD and UD songs from a single stimulus male as well as modified
972 versions of the song (mFD and mCTRL). The order of stimulus presentation was randomized for each
973 female. Sound was recorded continuously throughout the entire period of testing using SAP.

974 The number of calls in the pre-stimulus and stimulus period were counted manually, by a person blind to
975 the experimental conditions, using custom written Matlab routines (~~Mathworks, Natick, MA~~). No
976 distinction was made between call types. To assess females' responses to the different song types, we
977 calculated the percent change in call-back behavior in response to the stimulus playback (% call-back):

978
$$\% \text{ call - back} = \frac{\text{calls}_{\text{stimulus}} - \text{calls}_{\text{pre-stimulus}}}{\text{calls}_{\text{stimulus}} + \text{calls}_{\text{pre-stimulus}}}$$

979 A positive value for the % call-back indicates thus an increase in calling after presentation of the song as
980 compared to the pre-stimulus period, whereas a negative value indicates a decrease in calling.

981 **Quantification and statistical analysis**

982 **fMRI group analysis**

983 Statistical voxel-based group analysis of the fMRI data was done in SPM12 (Wellcome Trust Centre for
984 Neuroimaging, London, UK; <http://www.fil.ion.ucl.ac.uk/spm>). The Family Wise Error (FWE) method was
985 applied to adjust p-values to the number of independent tests performed. This method uses the Random
986 Field Theory to calculate the number of independent tests, taking into account the number of voxels as
987 well as the amount of auto-correlation among the data. Data were considered significant for $p_{\text{FWE}} < 0.05$
988 with a minimal cluster size of 5 voxels. For whole brain analyses, FWE correction appeared too
989 conservative to detect any effects, therefore, in such analyses a statistical threshold of $p < 0.001$ without
990 any correction for multiple comparisons (p_{uncorr}) was applied with a minimal cluster size of 10 voxels but
991 without any correction for multiple comparisons (p_{uncorr}). Reflecting the voxel basis of the analysis, results
992 are reported by the highest voxel T value within each cluster (T_{max}) and the associated voxel p-value.

993 In a first stage of the group analysis, we considered only the response to FD and UD song in order to
994 determine the selective neural substrates of FD song perception at the level of the whole brain. For this,
995 we entered the single subject t-contrast images for FD song > rest and UD song > rest into a paired t-test
996 design for FD > UD song. Subsequently, we converted these FD song selective clusters (using a significance
997 level of $p_{\text{uncorr}} < 0.001$) into regions of interest (ROIs) for further in depth analysis.

998 In a second stage, we considered data from both fMRI sessions to determine differential responses to
999 mFD or mCTRL versus FD and UD song stimulation within these ROIs. As these data originated from two
1000 separate fMRI time series as described above, we used the single subject t-contrast images with the pure
1001 tones as reference (used as identical reference stimulus in both sessions) in this analysis. Before including
1002 the pure tones as a reference in the analysis, we verified responses to this stimulus at the whole brain
1003 level by entering the single subject t-contrast images for pure tones > rest into a one sample t-test (see
1004 Figure S1A). For statistical analysis of the differences in response to mFD or mCTRL versus FD and UD song,
1005 we entered the individual single subject t-contrast images into a flexible factorial design with subjects as

1006 random variable. We explored the main effect of stimulus and performed individual t-tests to investigate
1007 the origin of the differences in the responses to the different stimuli. A statistical threshold of $p_{FWE} < 0.05$
1008 was applied with correction at the level of the respective ROIs.

1009 Besides voxel based group analysis, we also performed an ROI analysis to compare average responses
1010 between FD and UD song over hemispheres. For this, we performed a repeated measures ANOVA analysis
1011 with stimulus and hemisphere as within-subject factors using IBM SPSS Statistics for Windows (Version
1012 22.0. Armonk, NY: IBM Corp.). Bonferroni correction was applied for all post hoc tests with $\alpha < 0.05$.

1013 Finally, we also analyzed the responses to pure tones within both ROIs. Specifically, for the NCC and CMM,
1014 we used two mixed-effects models, one to test for differences between the stimuli and a second to test
1015 for differences between the hemispheres. In both cases, BOLD response was the dependent variable and
1016 bird ID was included as a random variable. We used Tukey's HSD (honest significant difference) test for all
1017 post-hoc tests with $\alpha < 0.05$ unless otherwise noted.

1018 **EGR1 expression analysis**

1019 We analyzed whether stimulus context (FD vs. UD song) influenced EGR1 expression in the CMM and the
1020 NCC. We first checked for the normality of the raw data and the residuals by looking at the linearity of
1021 quantile-quantile plots and fitting a normal curve to the distribution followed by a Shapiro-Wilk W test of
1022 the goodness of fit of the curves. If data or residuals were non-normally distributed, we performed data
1023 transformations to improve normality. Here, we report the results for log transformed data, although box-
1024 cox transformations were similarly effective. We then used a mixed-effects model with stimulus context
1025 (FD vs. UD song), hemisphere (left vs. right), and the interaction as the independent variables and batch
1026 and bird ID nested within batch as random variables. We analyzed the number of EGR1-ir cells/mm², or
1027 the log number of EGR1-ir cells/mm², as the dependent variable. Unbounded variance components were
1028 used and the restricted maximum likelihood method was applied to fit the data. We found no significant
1029 interaction between stimulus context and hemisphere in any of the brain regions and thus report only the
1030 results for the main effects of stimulus context and hemisphere. Silent controls were not included in the
1031 statistical analyses but are presented in the figures to allow visual comparison. We performed the
1032 statistical analysis in JMP® (Version 13, SAS Institute Inc., Cary, NC, 1989-2007) and used Tukey's HSD
1033 (honest significant difference) test for all post-hoc tests with $\alpha < 0.05$ unless otherwise noted.

1034 **Call-back analysis**

1035 We investigated the differences in call-back to the different stimuli using a mixed-effects model with
1036 unbounded variance components and the restricted maximum likelihood method to fit the data. % call-
1037 back was analyzed as the dependent variable while female ID was included as a random variable. The
1038 analysis was performed in JMP® (Version 13, SAS Institute Inc., Cary, NC, 1989-2007) and we used Tukey's
1039 HSD test for all post hoc tests with $\alpha < 0.05$ unless otherwise noted.

1040 We also analyzed variation in the ranking of the four stimuli. In particular, we noted that while most
1041 females exhibited the greatest increases in calling to FD song, the responses to the other three stimuli
1042 were generally both lower and more variable. To analyze these differences, we ranked the responses of
1043 each bird to the four stimuli, with 1 indicating the most positive response and 4 as the most negative
1044 response. In the event of a tie, more than one stimulus could receive the same ranking. We then
1045 performed a contingency analysis with stimulus type as the independent variable, ranking as the ordinal
1046 dependent variable, and bird ID as a third classification variable to account for repeated measures. We
1047 used the Cochran Mantel Haenszel χ^2 tests to compare all pairs of stimuli to test for linear relationships
1048 between stimulus and ranking across bird IDs.

1049 **Key resources table**

1050 See separate document

1051 **Data availability**

1052 [Datasets for the counts of EGR1 cells and the results of the callback behavior assays are available at](#) .

1053 All [other](#) data are available upon request to the authors.

1054